Journal of Applied Phycology (2022) 34:3157–3175
https://doi.org/10.1007/s10811-022-02832-w

Purification, characterization and assessment of stability, reactive oxygen species scavenging and antioxidative potentials of mycosporine-like amino acids (MAAs) isolated from cyanobacteria

Deepak K. Singh[1,2] · Jainendra Pathak[1,3] · Abha Pandey[1,4] · Rajneesh[1] · Vidya Singh[1,5] · Rajeshwar P. Sinha[1]

Received: 23 June 2022 / Revised and accepted: 30 August 2022 / Published online: 19 September 2022

Abstract
Mycosporine-like amino acids (MAAs) were characterized and their stability and free radical scavenging potentials were investigated in *Anabaena* sp. HKAR-7 and *Fischerella* sp. AR-5. UV/VIS absorption spectroscopy, high performance liquid chromatography and electrospray ionization-mass spectrometry showed occurrence of diverse forms of MAAs at retention time (RT) 1.16 (shinorine), 2.18 (mycosporine glycine-310) and 3.14 min (palythinol) with UVλ_{max} 310, 332 and 334 nm respectively, in *Fischerella* sp. when contrasted with *Anabaena* sp. (prominent peak at RT 3.21 min (porphyra 334; P-334) with UVλ_{max} 334 nm. MAAs showed dose-dependent in vitro antioxidative and in vivo reactive oxygen species (ROS) scavenging potentials. The MAA P-334 was used against strong allelochemical pyrogallic acid in *Anabaena* sp. P-334 reducing the negative impacts brought about by ROS, in this way, the malondialdehyde content and unwinding of dsDNA were similarly low. This clarifies the role of MAA P-334 against cell's ROS under studied stressed conditions.

Keywords Antioxidants · Allelochemical · Cyanobacteria · Mycosporine-like amino acids · Reactive oxygen species · Ultraviolet radiation

Introduction

The Gram-negative prokaryotes, the cyanobacteria constitute a heterogeneous assemblage of oxygen-evolving photosynthetic living organisms having cosmopolitan distribution (Stanier and Cohen-Bazire 1977). They appeared on the Earth in the time of the Precambrian period ($2.8–3.5 \times 10^9$ years ago) and gave a favorable situation to the current oxidized atmosphere (Fischer 2008; Pathak et al. 2021). Cyanobacteria are significant biomass producers (Häder et al. 2007) and possess a central position in nutrient cycling of biological systems. Secondary metabolites derived from cyanobacteria have pharmaceutical qualities (Rastogi and Sinha 2009; Rajneesh et al. 2017a; Singh et al. 2020a, b). Apart from having potential for biotechnological applications in the field of biofertilizers, fuel, food, biomedicals and mariculture (Richa et al. 2011; Singh et al. 2016; Pathak et al. 2018), cyanobacteria serve as crucial model organisms in photosynthetic experiments, partly due to their prokaryotic cellular organization (Olsson-Francis et al. 2013).

The presence of the ozone layer in the stratosphere protects living beings on the Earth from the lethal ultraviolet radiation (UVR) (Weatherhead and Andersen 2006). This layer is being depleted tremendously due to anthropogenic air pollutants such as chlorofluorocarbons, organobromides, and chlorocarbons, prompting the ozone holes (Crutzen 1992). Increased sunlight based UVR is a significant stress factor for prokaryotic as well

✉ Rajeshwar P. Sinha
rpsinhabhu@gmail.com

1 Laboratory of Photobiology and Molecular Microbiology, Centre of Advanced Study in Botany, Institute of Science, Banaras Hindu University, Varanasi 221005, India

2 Department of Botany, A.N.D. Kisan P.G. College, Babhnan, Gonda Affiliated to Dr. Ram Manohar Lohia Avadh University, Faizabad 271313, India

3 Department of Botany, Pt. Jawaharlal Nehru College, Banda Affiliated to Bundelkhand University, Jhansi 210001, India

4 Department of Botany, Swami Shraddhanand College (University of Delhi) Alipur, Delhi 110036, India

5 Department of Botany, Government PG College, Kuchhechha, Hamirpur Affiliated to Bundelkhand University, Jhansi 210301, India

as eukaryotic phytoplankton (Manney et al. 2011; Richa et al. 2016). Cyanobacteria are exposed to deadly doses of ultraviolet-B (UV-B, 280–315 nm) and ultraviolet-A (UV-A, 315–400 nm) radiation in their common brightly lit habitats (Rajneesh et al. 2019). Although just a little UV-B (under 1% of the gross solar radiation) reaches to the Earth's surface, it is extremely damaging for biological system as it can be absorbed by significant biomolecules such as nucleic acids, lipids and proteins ultimately having an adverse impact on living system (Karentz et al. 1991; He and Häder 2002a; Jantaro et al. 2011; Rajneesh et al. 2019). The UV-B radiation with high energy has considerable potential for cell impairment with direct consequences to DNA and proteins and indirect impacts via the generation of reactive oxygen species (ROS) (Rajneesh et al. 2019; Ahmed et al. 2021a; Singh et al. 2022). UVR effectively impacts different life processes in cyanobacteria, such as survival, growth and development, morphology, pigmentation, cell separation (differentiation), motility and orientation, phycobiliprotein composition, N_2 fixation, protein profile, CO_2 uptake and DNA damage (Gao et al. 2007a, b; Lesser 2008; Kannaujiya and Sinha 2015; Singh et al. 2017a, b; Pathak et al. 2019; Kumar et al. 2020).

In aquatic environments cyanobacterial blooms are a major cause of concern and occur frequently worldwide. The process of bloom formation is aggravated by enhanced eutrophication of water bodies (Shao et al. 2009; Mayer et al. 2011), leading to the deterioration of water quality as these algae produce toxins, scum, hypoxia and also result in bad tastes and odors of the water (Codd et al. 2005). Hence, controlling these algal blooms is an important area of research and naturally occurring allelochemicals could serve as better approach for controlling harmful cyanobacterial blooms compared to physical and chemical methods because of their environment friendly nature (Melzer 1999; Vanderstukken et al. 2011). *Myriophyllum spicatum* has significant inhibitory effects on the major bloom and toxin producing cyanobacterium *Microcystis aeruginosa* allelopathically (Nakai et al. 2000). Four allelochemicals which were polyphenol in nature, namely, pyrogallic acid (PA), ellagic acid, gallic acid and (+)-catechin were identified in the culture solution of *M. spicatum*. Studies showed that these polyphenolic compounds exert their inhibitory effects on algae by suppressing the activities of alkaline phosphatase and attacking photosystem II (PSII) of *M. aeruginosa* leading to oxidative damage in the cells (Gross et al. 1996; Leu et al. 2002; Zhu et al. 2010; Wang et al. 2011). As a well-known biologically active compound with widespread occurrence in aquatic macrophytes, PA is regarded as the most promising of such compounds. However, there is a scarcity of information regading the mechanism of action of PA on cyanobacterial species together with exogenous supplements of mycosporine-like amino acids (MAAs).

Cyanobacteria are a valuable source of various natural products of medicinal and industrial importance (Sinha and Häder 2008; Rastogi and Sinha 2009; Rajneesh et al. 2017a; Singh et al. 2021) sythesising numerous secondary metabolites. MAAs, scytonemin, carotenoids and a few other UV-absorbing substances have been recognized from different groups of organisms (Pathak et al. 2017, 2020; Pandey et al. 2020; Ahmed et al. 2021a, b). MAAs absorb essentially in the UV-B (280–315 nm) and UV-A (315–400 nm) range, and this helps these organisms to develop and survive in environments exposed to intense solar radiation (Sinha and Häder 2008; Singh et al. 2010; Rastogi and Incharoensakdi 2013; Rastogi et al. 2014). The distribution of MAAs varies from tropical to polar regions in various groups of organisms (Shick and Dunlap 2002), but these compounds are typically present in organisms such as cyanobacteria and other prokaryotes and eukaryotic microorganisms such as microalgae, fungi, lichens, marine macroalgae, corals, and other marine organisms which are exposed to UVR/high-intensity radiation (Shibata 1969). Some of these organisms accumulate MAAs from their feed via the food chain (Sinha et al. 2007; Pandey et al. 2017). In terms of biosynthesis, accumulation, and metabolism of MAAs, the Nostocales is the most investigated group (Jain et al. 2017). Furthermore, until now no MAAs have been reported in the cyanobacterial orders Gloebacterales, Chroococcidiopsidales, Pleurocapsales and Spirulinales (Jain et al. 2017). Techniques, such as, ultraviolet–visible (UV–VIS) spectroscopy, Fourier-transform infrared (FTIR) spectroscopy, nuclear magnetic resonance (NMR) spectroscopy and electrospray ionization mass spectrometry (ESI–MS) are quick and high-resolution separation detection systems, with high-throughput (Dunn et al. 2005). High-performance liquid chromatography (HPLC)-based profiling of MAAs in cyanobacteria is well documented (Matsui et al. 2011; Rastogi and Incharoensakdi 2014; Hu et al. 2015). NMR spin-relaxation times data after NMR spectroscopy help in the characterization of MAAs (Burja et al. 2003). Torres et al. (2006) have reported the structure and molecular formula of porphyra-334 (P-334) by the application of mass spectroscopy (MS) in conjunction with ^{1}H and ^{13}C NMR data. Moreover, different functional groups in P-334 were determined by FTIR analysis of the purified MAA (Richa and Sinha 2015).

MAAs show stability under various abiotic stressors, such as, heat, UV-B, H_2O_2, and pH (Rastogi et al. 2016), which makes them suitable to be used as a sunscreen. The wide diversity,distribution, photoprotection and physicochemical stability of MAAs make them an important class of UV-screening compounds and future investigations must be focused on biosynthesis, profiling, and characterization of these sunscreens.

In the present study we screened and characterized MAAs in two cyanobacteria, *Fischerella* sp. HKAR-5 and *Anabaena* sp. HKAR-7, from different habitats. Furthermore,

we assessed the stability, antioxidant and ROS scavenging potentials of selected MAAs as well as their role in reduction of UVR-induced formation of ROS. We also studied the effects of P-334 against different doses of strong allelochemical PA in *Anabaena* sp. HKAR-7. Induction and screening of UV-protective compounds (MAAs) was studied in both cyanobacteria under different combination of exposure to photosynthetically active radiation (PAR), PAR + UV-A, PAR + UV-B and PAR + UV-A + UV-B radiation.

Materials and methods

Culture methods and maintenance

BG-11 (-) medium (BG-11 minus nitrogen) was used for the culture of the cyanobacteria (Rippka et al. 1979). The cultures were regularly grown under axenic conditions, in a culture room at 28 ± 2 °C, under fluorescent white light (12 W m^{-2}). The cultures were hand-shaken 3–4 times a day for avoiding clumping and shelf shading.

Growth measurement

Growth of cyanobacteria was determined by determining the changes in chlorophyll *a* (Chl *a*) content and optical density (O.D.) at 750 nm.

UV irradiation and exogenous supplements

The test cultures were exposed to artificial UVR in a chamber designed with UV-tubes (UV-chamber). During UVR exposure, the test samples were simultaneously irradiated with cool white fluorescent light (12 ± 1.0 W m^{-2}). The homogeneous cultures (250 mL of culture in each Petri dish with OD_{750} nm = 0.68 ± 0.5; path length 1 cm) were treated with UVR or PA in Petri dishes (replicate of three) for the desired time intervals. Petri dishes were covered with 395, 320 and 295 nm cut-off filter foils (Ultraphan; Digefra, Germany) to ensure PAR, PAR + UV-A, PAR + UV-B and PAR + UV-A + UV-B radiation exposure respectively. A constant temperature of 23 ± 2 °C was maintained in all experimental cultures in UV-chamber to avoid heating effects. The cultures were shaken continuously during experiments. White fluorescent light illuminated samples served as control. All the trials were carried out in the exponential phase of cultures with OD_{750} of ~ 0.75 to 0.85.

Percent survival

For estimation of survival percentage, 100 µL aliquots from each treated culture were withdrawn at the desired time and plated on agar plates. Treated plates were incubated in the dark for 48 h and then transferred to light in the culture room. After 12–15 days of growth colonies were counted and percentage survival was determined.

Protein estimation

Protein estimation was according to Bradford (1976). Bovine serum albumin (BSA) was utilized as the standard.

Pigments estimation

The chlorophyll (Chl *a*) was extracted in methanol. The harvested cyanobacterial sample was kept in 100% methanol for overnight in the dark at 4 °C and the Chl *a* content was determined according to Porra (2002):

$$\text{Chl a}\left(\mu\text{g mL}^{-1}\right) = 16.29 * A_{665.2} - 8.54 * A_{652}$$

Carotenoid content was determined following the method of Jensen (1978) with slight change. In brief, homogenized culture suspension was centrifuged at 5000 × *g* for 10 min and the supernatant discarded. The macerated pellet was placed in 85% acetone and incubated overnight.Carotenoids were determined by measuring the O.D. at 450 nm. For estimation of phycocyanin (PC), cyanobacterial cells were harvested by centrifugation (5000 × *g* for 10 min) at room temperature and cells were washed with 50 mM phosphate buffer (pH 7.0). Thereafter, cells were resuspended in a minimal amount of the same buffer with addition of 1 mM phenylmethanesulfonylfluoride (PMSF), 10% (w/v) EDTA and 5% (w/v) sucrose. Cells were sonicated for 3–5 min and the resulting suspension was subjected to repeated freeze–thaw cycles at -20 and 4 °C, respectively. The cell debris was removed by centrifugation at 15,000 × *g* for 30 min and the supernatant was considered as partially purified phycobiliproteins. Spectra were recorded at 200–700 nm against phosphate buffer. The PC content was calculated using equation described by Bryant et al. (1979).

$$\text{PC}\left(\text{mg mL}^{-1}\right) = \left\{\left(A_{620} - \left(0.7 * A_{650}\right)\right\}/7.38$$

Photosynthetic activity assay

The pulse amplitude modulation (PAM) fluorometer technique was used to determine the maximum photochemical efficiency (quantum yield) of open reaction centre (RC) IIs (F_v/F_m) by using PAM fluorometer (PAM-2500, Heinz Walz GmbH, Germany). The treated cyanobacterial samples were dark-adapted for 30 min to allow complete oxidation of PSII reaction centers and the minimum (F_0) and maximum (F_m) fluorescent yields of PSII in the dark-adapted state were determined and used to calculate the F_v/F_m by the formula as described by Genty et al. (1989) and (Cosgrove

and Borowitzka 2011). Estimation of the maximim relative electon transport rate ($rETR_{max}$) was done from the operational PSII photochemical yield measured at different photosynthetic photon flux densities (PPFDs) (Cosgrove and Borowitzka 2011).

$$rETR_{max} = F_q'/F_m' \times 0.5 \times PPFD$$

where F_q'/F_m' denotes the effective photochemical efficiency of reaction center II (RCII) in actinic light.

MAAs extraction and partial purification

Extraction and purification of MAAs was done by UV–Vis spectroscopy and HPLC as per (Rastogi and Incharoensakdi 2013) with slight modification. Briefly, irradiated cyanobacterial samples were centrifuged and pellets were extracted in 5.0 mL of 100% (v/v) HPLC-grade methanol and incubated overnight at 4 °C. Thereafter, the aliquots were centrifuged (8,000 × *g* for 10 min) and the supernatant (methanolic extract) was spectroscopically analyzed (UV–Vis 2900, Hitachi, Japan). The methanolic extracts were dried at 45 °C and re-dissolved in 1 mL double distilled water and again absorption spectra were recorded. The samples were filtered through 0.2 µm pore-sized small-scale centrifuge filters for HPLC examination (Waters 2998, pump L-7100, Photodiode Array, USA with Waters, Spherisorb diagnostic column, 5 µm, 4.6×250 mm diameter, a Licrospher RP 18 column and guard. MAAs assessment was completed by injecting the samples into the HPLC through a Waters 717 plus autosampler. The mobile phase was 0.02% acetic acid (v/v) in double distilled water at a flow rate of 1.0 mL min^{-1} (Richa and Sinha 2015). The MAAs was identified by comparing previously published information dependent on absorption spectra and RT. The extracted MAAs were analyzed and separated by using the HPLC system and subsequently, the partially purified MAAs were subjected to characterization, stability and antioxidant function assays.

Biochemical characterization of MAAs

Electrospray ionization-mass spectrometry (ESI–MS) MAAs collected from HPLC were subjected to ESI–MS to produce protonated molecules. Mass spectra were recorded on an Amazon SL mass spectrometer (Bruker Daltonics Inc., Germany). Cone voltage of 30 V was found to induce the formation of $(M+H)^{1+}$ with a mass range of 100–1,000 m/z. Data were analyzed using the software Data Analysis 4.0 (Bruker Daltonics Inc).

Fourier transform infrared (FTIR) spectroscopy MAAs isolated from the HPLC system werelyophilized and combined with oven-dried potassium bromide in a 1:100 ratio. Transparent disk was prepared for FTIR examination and spectra were recorded in a Perkin Elmer Infrared Spectrophotometer version10 (USA).

Nuclear magnetic resonance (NMR) spectroscopy The purified MAAs were dissolved in 5 mg mL^{-1} D_2O (isotopic purity: 99.5 atoms) after lyophilization. Room temperature ^1H and ^{13}C NMR spectra were recorded with a With the assistance of theJEOL AL300 FTNMR spectrometer (JEOL Ltd., Tokyo, Japan).

CHNS analysis The composition ratio of organic carbon, hydrogen, and nitrogen was determined in a CHNS Elemental Analyzer (EURO EA 3000, EuroVector S.P.A., Italy).

Stability of MAAs

Stability of MAAs was observed under different abiotic stressors such as UVR (PAR, PAR + UV-A, PAR + UV-A + UV-B), heat (-20, 4, 25 and 60 °C), pH (1, 3, 7, 9 and 12) and H_2O_2 (strong oxidizing agent) (0.1, 0.25 and 0.50%). The purified MAAs was treated with different pH and variable concentration of H_2O_2 for 5 h and their effects were analyzed at 1, 3 and 5 h intervals. For the heat treatment, MAAs were exposed at variable temperature until 45 days of exposure.The treated MAAs samples were assessed after 15, 30 and 45 days of exposure. In the radiation experiment, purified MAA were exposed to different combinations of radiation by using different cutoff filters of 395 nm (PAR), 320 nm (PAR + UV-A) and 295 nm (PAR + UV-A + UV-B) for 7 days in the UV-induction chamber. Samples were analyzed at of 1, 3, 5 and 7 days of exposure. A sample without any exposures served as control.

Free radical scavenging activity of MAAs

The antioxidant capacity of purified MAAs, P-334 and MG-310 at different diluted concentrations (stock 100 µg mL^{-1}) of 0, 20, 40, 60, 80 and 100 µL was measured by performing DPPH, SRSA and RP assaya. Determination of free radical scavenging capacity of purified MAAs was done in comparison to ascorbic acid (AA).

2,2-diphenyl-1-picryl-hydrazyl (DPPH) assay The free-radical scavenging activities by DPPH assay were assessed according to Kulisic et al. (2004) and Rastogi et al. (2016) with slight changes. Briefly, both MAAs, P-334 and MG-310 with different doses were kept with 0.1 mM DPPH in 80% methanol for 1 h in the dark at room temperature. The sample without any MAAs concentration (only DPPH solution) served as control. The optical density of each reaction mixture was determined at 517 nm. The DPPH radical

scavenging potential (%) for each concentration of test samples of MAAs were determined using the equation (Rastogi et al. 2016):

$$\text{DPPH radical scavenging capacity } (\%) = \left[\left(A_1 - A_2\right)/A_1\right] \times 100$$

where A_1 = absorbance at 517 nm of control (DPPH solution) and A_2 = absorbance at 517 nm of samples (MAAs + DPPH).

Superoxide radical scavenging activity (SRSA) assay The SRSA assay was performed by the modified method of Li (2012) and Rastogi et al. (2016). SRSA action depends on pyrogallol autoxidation. The percentage of SRSA was determined by the equation:

$$\text{SRSA}(\%) = \left[\left(\Delta A_1\right) - \left(\Delta A_2\right)/\left(\Delta A_1\right)\right] \times 100$$

where ΔA_1 = change in the absorbance (A_{325}) of control and ΔA_2 = change in the absorbance(A_{325}) of samples.

Reducing power (RP) assay Purified MAAs were used to determine their reducing potential by the methods of Oyaizu (1986) and Rastogi et al. (2016). Ascorbic acid was utilized as standard. Various concentrations of MAAs (P-334 and MG-310) were mixed with buffer solution (200 µL) of 0.2 M sodium phosphate at pH 6.6 containing 1% potassium ferricyanide. The mixture was incubated and then 10% trichloroacetic acid (200 µL) was added. An equivalent quantity of water was mixed with the reaction mixture and 120 µL of 0.1% ferric chloride was added. After 10 min reaction, the absorbance was recorded at 700 nm.

ROS detection by fluorescence spectrophotometry and fluorescence microscopy

The fluorimetric probe dichloro-dihydro-fluorescein diacetate (DCFH-DA) was utilized to observe the ROS level in the cyanobacterial cells (Rastogi et al. 2010). DCFH-DA at a concentration of 5 µM was used. The fluorescence intensity of the treated samples was determined with a a fluorescence spectrophotometer (Cary Eclipse, Agilent Technologies) with an excitation wavelength of 485 nm and an emission band at 525 nm at room temperature. To observe fluorescence the treated samples were analyzed by utilizing a Nikon eclipse Ni fluorescence microscope equipped with NIS-Elements (BR) imaging software. Fluorescence intensities of green (G) and red (R) were acquired for arbitrarily chosen regions on the cyanobacterial filaments. The ratio G/R and fluorescence intensity was observed for the chosen region by using the software provided by the manufacturer (Rajneesh et al. 2017b).

Determination of antioxidant enzyme activity

To assay the changes occurring in the concentration of antioxidant enzymes during course of experiment, cell extracts were prepared after sonication in an extraction mix containing 50 mM phosphate buffer (pH 7.5), 2.5 mM phenylmethanesulfonyl fluoride (PMSF), 1 mM ethylenediaminetetraacetic acid (EDTA) and 1% (w/v) polyvinylpyrrolidone (PVP). The extraction suspension was sonicated (Sonic and Materials, USA) and centrifuged at 10,000 × *g* for 25 min at 4 °C. The supernatant was used for the analysis of enzymes.

Catalase (CAT) activity CAT activity was determined by the method of Rao et al. (1996). Reaction mixtures contained 2.86 mL phosphate buffer (pH 7.5), 4.4 mM H_2O_2 and 100 µL of enzyme extract. CAT activity was observed by recording absorbance at 240 nm. CAT activity measures the extent of O_2 release from enzymatic dissociation of H_2O_2 in darkness for 5 min.

Superoxide dismutase assay (SOD) SOD assay measures the inhibition in the photochemical reduction of nitroblue tetrazolium (NBT). The reaction product was measured at 560 nm (Donahue et al. 1997). The reaction mixture of 2.1 mL contained 1.5 mL, 0.1 mM EDTA, 13 mM Met, 75 µm nitroblue tetrazolium and 2 µm riboflavin in 50 mM phosphate buffer (pH 7.8) and 600 µL of cell extract. Riboflavin was added last and the reaction was initiated by placing the tubes under two 15 W m^{-2} fluorescent lamps. The reaction was terminated after 10 min by removal from the light source.

DNA extraction and gel electrophoresis

DNA extraction was by the method of Sinha et al. (2001a). Briefly, cyanobacterial pellet was washed 2–3 times with of STE buffer (1 mL) (50 mM Tris–HCl (pH—8.0) + 50 mM NaCl + 5 mM EDTA) subsequently re-suspended in a TE (500 µL) buffer (50 mM Tris–HCl (pH—8.0) + 50 mM EDTA). Buffer containing pellet was sonicated for 5 min on ice. Then the cyanobacterial filaments were treated with proteinase K (100 µg mL^{-1}). The extraction buffer consists of 3% (w/v) CTAB + 1% (w/v) sarkosyl + 20 mM EDTA + 1.4 M NaCl + 0.1 M Tris–HCl, pH—8.0 + 1% (w/v) 2-mercaptoethanol). Prewarmed extraction buffer (750 µL) was mixed and the sample incubated for 1 h at 55 °C in a water bath. Then formed suspension was cooled for few minutes and then chilled chloroform: isoamyl alcohol (24:1, v/v) of equivalent volume was added and gently mixed to form an emulsion. The emulsion was centrifuged (10,000 × *g* for 10 min) and the supernatant was transferred to sterile microcentrifuge tubes. Subsequently, ethanol and 3 M sodium acetate (pH—5.2) in ratio of 2

volumes and 0.1 volume were added, mixed gently and kept overnight at -20 °C for DNA precipitation. The the sample was centrifuged at 8,000 × *g* for 15 min at 4 °C and the supernatant decanted. The pellet was rinsed once with chilled 70% ethanol, dried and re-hydrated with 30 mL TE buffer (10 mM Tris–HCl (pH—8.0) + 1 mM EDTA). DNA purity was assessed by the A_{260}/A_{280} ratio (pure DNA preparations have A_{260}/A_{280} value of 1.8). DNA integrity was checked by sample (5 µL aliquot) resolved on agarose gel (0.8%). Equivalent measures of DNA stained with Gel Red were separated by electrophoresis on a 1.5% TBE agarose gel at 60 V for 90 min, and visualization of bands were done by utilizing the Bio-Rad Imaging System.

Malondialdehyde (MDA) content

MDA content was measured using the protocol described by Chen et al. (2009). Briefly, centrifuged cultures were homogenized with 10 mL 10% trichloroacetic acid (TCA). Then the culture was centrifuged at 6000 × *g* for 15 min and the supernatant (2 mL) was added to 2 mL 0.6% (w/v) thiobarbituric acid (TBA) and incubated in warm bubbling water for 12 min. The sample was again centrifuged at 10,000 × *g* for 10 min and the spectrum of the supernatant was recorded.

dsDNA breaks

DNA strand breaks were determined by fluorometric investigation of DNA unwinding (FADU) as descrtibed by He and Häder (2002b).

Results

UV-induced biosynthesis of photoprotective compounds (MAAs)

The cyanobacteria *Anabaena* sp. HKAR-7 and *Fischerella* sp. HKAR-5 were irradiated under different combinations of radiation i.e., PAR, PAR + UV-A, PAR + UV-B and PAR + UV-A + UV-B up to 72 h. In both cyanobacteria PAR + UV-A, PAR + UV-B and PAR + UV-A + UV-B were more effective wavebands for MAAs biosynthesis.

UV–Vis spectra and HPLC chromatogram of partially purified MAAs

Figure 1 depicts the absorption spectra of the partially purified MAAs. The HPLC chromatogram of MAAs from *Anabaena* sp. HKAR-7 showed a single prominent peak at RT 3.21 min with UVλ_{max} 334 nm (Fig. 2a, c) and *Fischerella* sp. HKAR-5 showed three peaks at RT 1.16, 2.18 and 3.14 min with UVλ_{max} 310, 332 and 334 nm, respectively (Fig. 2b, d).

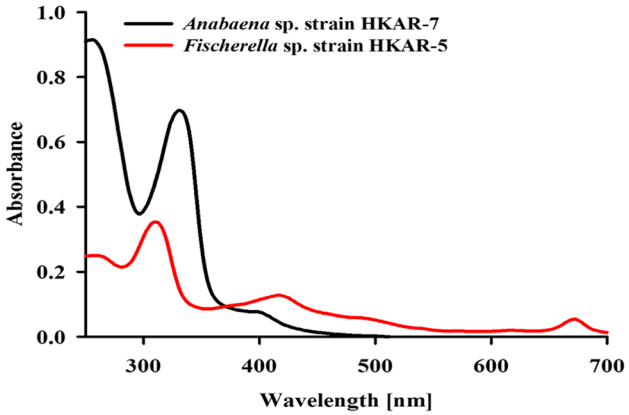

Fig. 1 UV–Vis absorption spectra of partially purified MAAs from *Anabaena* sp. strain HKAR-7 and *Fischerella* sp. HKAR-5

ESI–MS analysis

The HPLC separated fractions of each prominent peak were subjected to ESI–MS analysis. ESI–MS analysis revealed a prominent ion peak of protonated molecules $[M+H]^+$ at *m/z* 346.9 (Fig. 3a) from *Anabaena* sp. HKAR-7 and 333.1 (Fig. 3b), 246.4 (Fig. 3c) and 303.2 (Fig. 3d) from *Fischerella* sp. HKAR-5. Based on UV–Vis absorption spectra and MS, the single MAA, porphyra-334 (P-334) (λ_{max}: 334 nm, *m/z*346.9) was tentatively identified from *Anabaena* sp. HKAR-7. However, three MAAs, shinorine (λ_{max}: 334 nm, *m/z*333.1), mycosporine-glycine (MG-310) (λ_{max}: 309.6, *m/z*246.4) and palythinol (λ_{max}: 332, *m/z*303.2) were identified in *Fischerella* sp. HKAR-5 (Table 1). Among the five identified MAAs, the peak for P-334 from *Anabaena* sp. HKAR-7 and major peak for MG-310 from *Fischerella* sp. HKAR-5 were used for further characterization.

FTIR analysis

Purified and lyophilized MAAs samples were subjected to FTIR analysis to determine the presence of the functional groups. The FTIR wave motif of P-334 (from *Anabaena* sp. HKAR-7) demonstrated 3377.44, 2926.38, 2855.11, 2083.19, 1633.53, 1407.50, 1208.58, 1048.51 and 616.88 cm^{-1} bands indicating the presence of iminocyclohexene ring moiety, the center of MAAs (Takano et al. 1978) and indicated comparability with recently published reports for P-334 (Oyamada et al. 2008; Richa and Sinha 2015) (Supplementary Fig. 1a). Similarly, FTIR wave pattern of MG-310 (*Fischerella* sp. HKAR-5) gave frequency pattern with bands of 3403.10, 2925.26, 2854.47, 2270.23, 1743, 1628.04, 1461.60, 1074.79 and 606.29 cm^{-1} (Supplementary

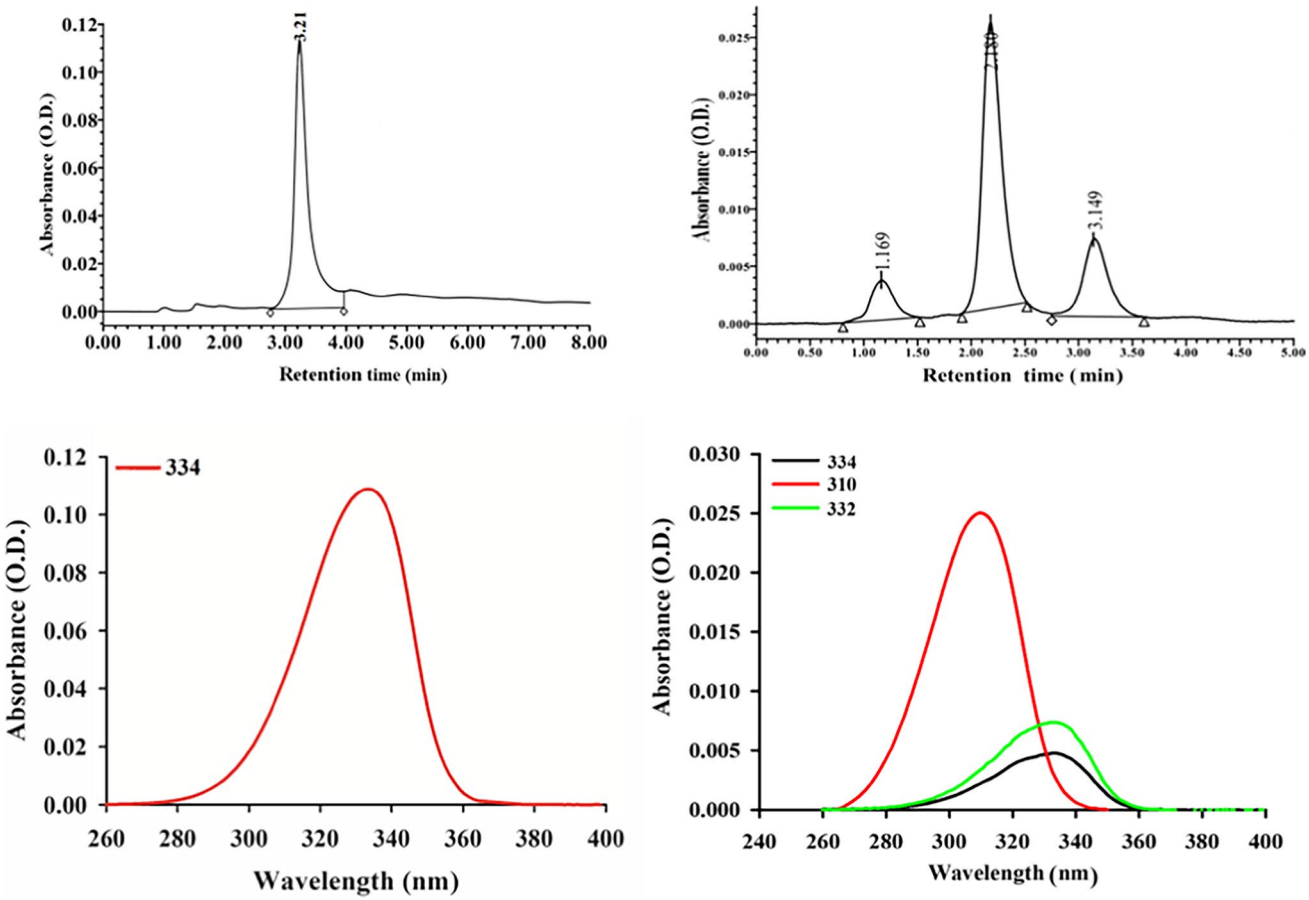

Fig. 2 HPLC chromatograms of MAAs and their corresponding absorption spectra in *Anabaena* sp. HKAR-7 (**a** and **c**) and *Fischerella* sp. HKAR-5 (**b** and **d**)

Fig. 1b) indicated the presence of MAA that resemble with MG-310 and quite similar to early published data (Singh et al. 2017a). Bands of 3377.44 cm^{-1}/3403.10 cm^{-1} might be of -OH functional group, 2926.38/2925.26 cm^{-1} for side-chain vibrations comprising of C-H stretching and showing the existence of -NH_2 functional group and 1633.53/1628.04 and 1407.50/1461.60 cm^{-1} bands might be assigned to the -NH_2 and carboxylic functional group, respectively. However, some additional different wave frequencies were also present in the P-334 wave pattern which make it different from MG-310.

Nuclear magnetic resonance (NMR) spectra analysis

The NMR spectra of purified fraction of MAAs, P-334 are shown in Supplementary Fig. 2a and b, and for MG-310 are shown in Supplementary Fig. 3a and b. The obtained data were correlated with recently published chemical shift information for P-334 (Oyamada et al. 2008; Yoshiki et al. 2009) and MG-310 (Singh et al. 2017a).

CHN analysis

Data obtained from the CHNS analyzer also supported the percentage composition of studied MAAs, P-334 and MG-310 (Table 2).

Stability of MAAs

In vitro stability of P-334 and MG-310 was studied under different physicochemical stressors. However, both MAAs showed resistance to most of the treatments. Among different exposure of stressors such as radiation (Fig. 4a), pH (Fig. 4b), strong oxidizing agent H_2O_2 (Fig. 4c) and variable temperature (Fig. 4d), higher concentrations of H_2O_2 (0.50%) had the most detrimental effects at later duration of incubation (5 h). Both MAAs showed similar trends of stability under different temperatures i.e. -20 °C, 4 °C, 25 °C and 60 °C. However, a significant decrease in concentration of MAAs was observed in the samples exposed to higher temperature i.e., 60 °C at 45 days exposure. In the radiation experiment, PAR + UV-A + UV-B exposure was the most

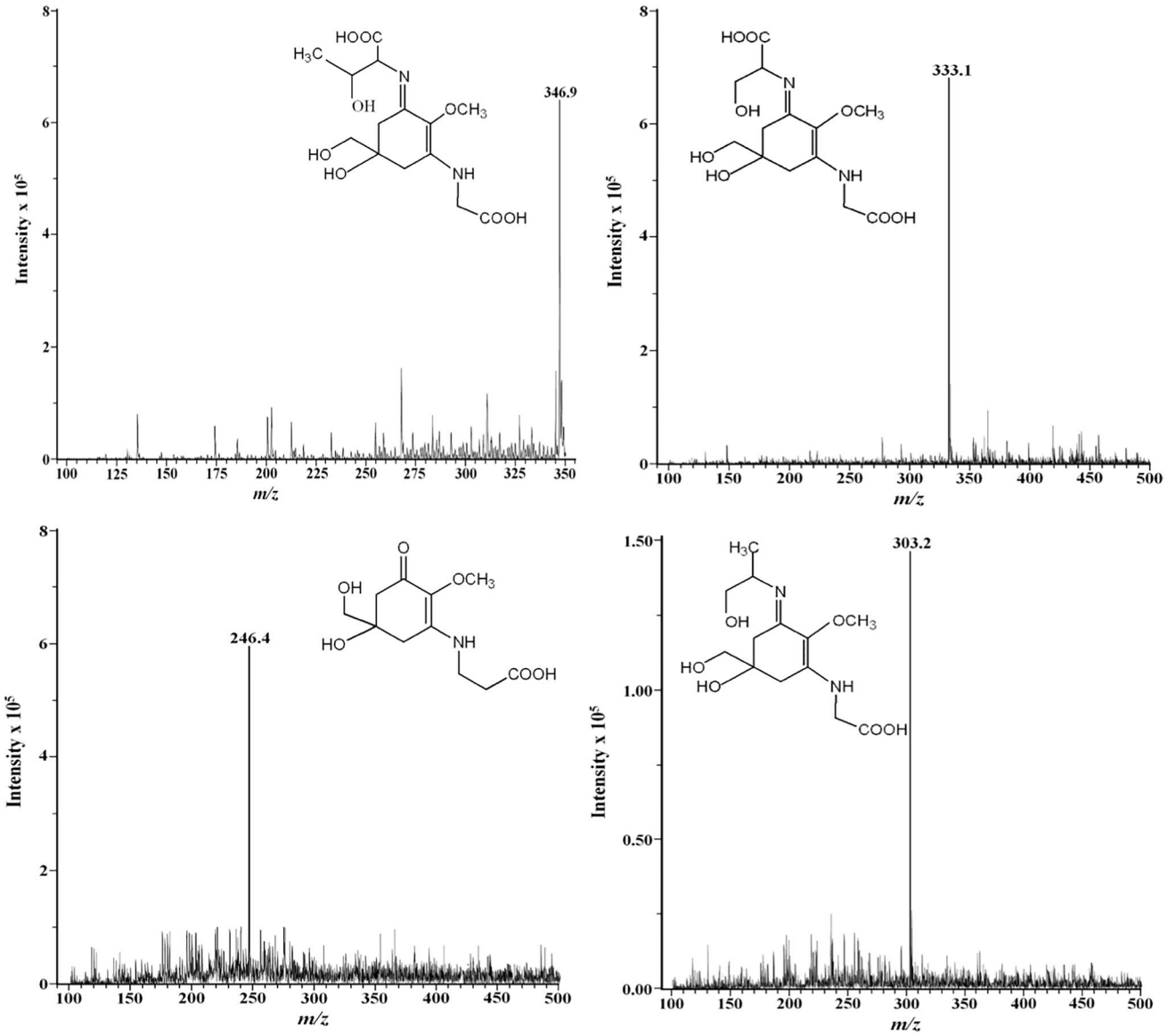

Fig. 3 Electrospray ionization-mass spectrometry of HPLC-purified MAAs. Porphyra 334; P-334 (**a**), shinorine (**b**), mycosporine glycine; MG-310 (**c**) and palythinol (**d**) showing peaks with *m/z* value of 346.9 (**a**), 333.1 (**b**), 246.4 (**c**) and 303.2 (**d**) respectively

Table 1 List of MAAs extracted from *Anabaena* sp. strain HKAR-7 and *Fischerella* sp. strain HKAR-5

Cyanobacteria	MAAs	Molecular formula	UVλ_{max} (nm)	RT (min)	m/z $[M+H]^+$
Anabaena sp. HKAR-7	P-334	$C_{14}H_{22}N_2O$	334	3.21	346.9
Fischerella sp. HKAR-5	Shinorine	$C_{13}H_{20}N_2O_8$	334	1.16	333.1
	MG-310	$C_{10}H_{15}NO_6$	309.6	2.18	246.4
	Palythinol	$C_{13}H_{22}N_2O_6$	332	3.14	303.2

effective waveband combination which resulted in a decrease in MAAs concentration after 7 days exposure. MAA samples with higher doses of an oxidizing agent like H_2O_2 (0.25 and 0.50%) showed the most detrimental effects with an enhanced duration of exposure (3 and 5 h). P-334 and MG-310 were quite stable in slightly acidic as well as neutral pH, however, their stability was affected by acidic (pH = 1) as well as highly basic medium (pH = 12) with a higher duration of exposure.

In vitro antioxidant capacity of MAAs

DPPH assay P-334 showed a dose-dependent DPPH-scavenging activity and the anti-oxidation was 20, 31, 42, 60

Table 2 Percentages of C, H and N of MAAs, P-334 and MG-310 (means ± SD, $n = 3$)

MAAs	%C	%H	%N
P-334	46.78 ± 2.50	5.15 ± 1.90	9.68 ± 1.63
MG-310	48.47 ± 2.10	4.80 ± 1.43	6.12 ± 2.20

and 90% and MG-310 exhibited 18, 25, 32, 52 and 84% at the doses of 20, 40, 60, 80 and 100 μL^{-1} MAA, respectively. However, 98% anti-oxidation was found at 100 μL^{-1} of ascorbic acid (Fig. 5a). IC_{50} estimations of P-334 and MG-310 against DPPH-radical are shown in Table 3.

SRSA assay UV-induced ROS may have consequences for cyanobacteria. Superoxide radicals (O_2^-) assume a significant role in lipid-peroxidation and thus, the biological role of MAAs in limiting the superoxide radicals (O_2^-) was studied. The superoxide radicals scavenging percentage was 18, 29, 45, 58 and 70% for P-334 and 14, 25, 41, 54 and 67% for MG-310 at concentrations of 20, 40, 60, 80 and 100 μL^{-1} MAAs, respectively (Fig. 5b). The IC_{50} values of P-334 and MG-310 against SRS assay are shown in Table 3.

RP assay Significant reducing capacity of MG-310 and P-334 was observed as indicated by the dose-dependent enhancement in the absorbance value at 700 nm (Fig. 6). The current outcomes demonstrated that MAAs act as strong antioxidative agent to prevent cellular damage occurring due to UV-induced ROS production.

In vivo ROS scavenging capacity of MAAs

Significant increase in levels of ROS was observed upon exposure to UV-B radiation. Significant decrease ($P < 0.05$) in fluorescence level of 2′,7′-dichlorofluorescein (DCF) was observed in the MAAs-treated cells exposed to UV-B radiation (Fig. 7a, b). These results were further confirmed by fluorescence pictures of *Anabaena* sp. HKAR-7 and *Fischerella* sp. HKAR-5 under various exposure conditions, for example, UV-B, UV-B + P-334, UV-B + MG-310 and

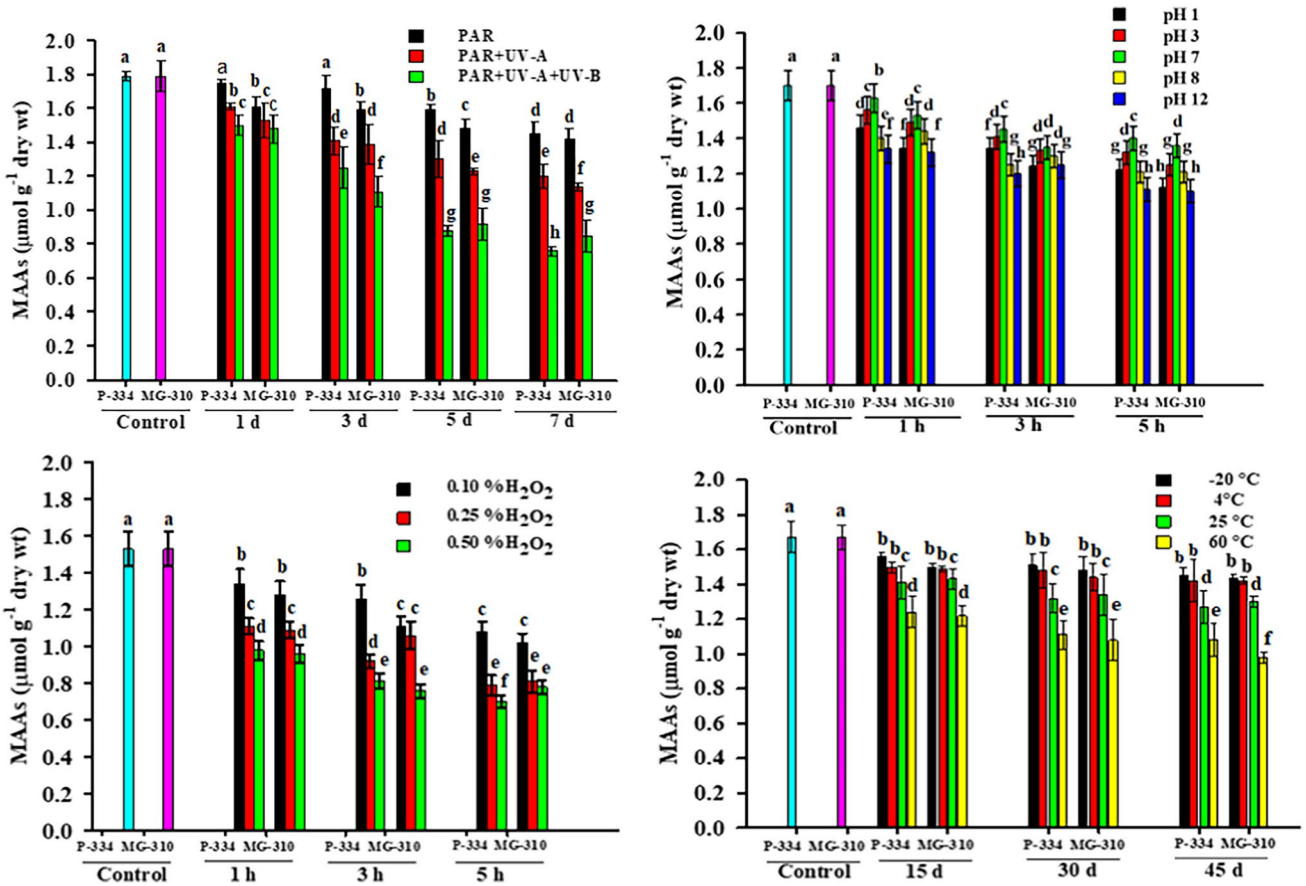

Fig. 4 Stability of porphyra-334 (P-334) and mycosporine glycine-310 (MG-310) under different abiotic stressors like radiations (Photosynthetically active radiation (PAR), PAR + UV-A, PAR + UV-A + UV-B) (**a**), pH (1, 3, 7, 9 and 12) (**b**), strong oxidizing agent H_2O_2 (0, 0.25 and 0.50%) (**c**) and temperature (-20, 4, 25 and 60 °C) (**d**). The error bars denote standard deviations of means ($n = 3$). Similar letters over bar represent homogeneous mean group ($p > 0.05$)

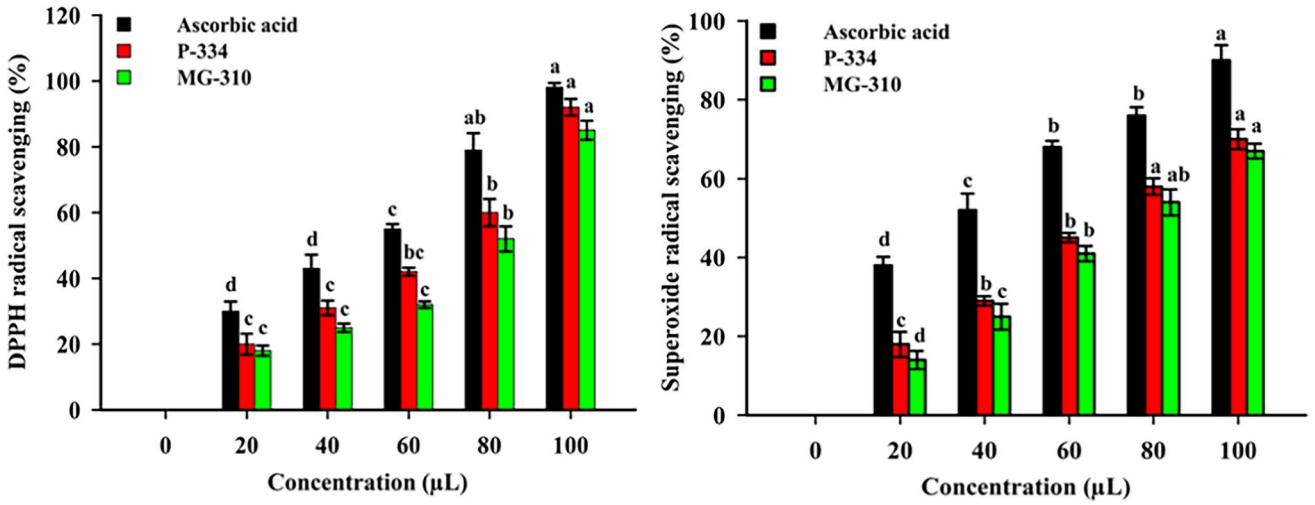

Fig. 5 Free radical scavenging capacity of MAAs, porphyra-334 (P-334) and mycosporine glycine-310 (MG-310) by 2,2-diphenyl-1-picryl-hydrazyl (DPPH) assay (**a**) and superoxide radical scavenging activity (SRSA) assay (**b**), correlated with that of ascorbic acid (AA). The error bars denote standard deviations of means ($n=3$). Similar letters over bar represent homogeneous mean group ($p>0.05$)

UV-B + P-334 + MG-310 after 12 h. Also, a diminished level of in vivo ROS in MAA-treated samples indicated the photoprotective capacity of MAAs against UV-induced oxidative stress. ROS scavenging capacity was observed maximum in the UV-B irradiated sample treated with P-334 and MG-310.

Role of exogenous supplement of P-334 against pyrogallic acid (PA) in *Anabaena* sp. HKAR-7

PA-induced growth inhibition The changes in percent survival of studied cyanobacterium were observed under different doses of PA (0, 5, 10, 20 and 50 mg L^{-1}) for 24 h (Fig. 8). Percent survival was inhibited under exposure of PA and the inhibition was dose and time-dependent. The number of colonies that appeared without any exposure of PA at 0 h served as control (untreated) and were considered as 100%. Cell survival (%) considerably declined in all treated samples until 24 h of exposure and a maximum decrease of 61% was observed in 50 mg L^{-1} PA treated culture at 24 h.

Table 3 IC_{50} estimations of P-334 and MG-310 and ascorbic acid for different oxygen species derived from various in vitro antioxidant tests. Data are expressed as means of percentage inhibition ± standard deviations of means ($n=3$)

Test	IC_{50} values (µg mL^{-1})		
	Ascorbic acid	P-334	MG-310
DPPH	56 ± 1.33	80 ± 3.13	85.2 ± 4.34
SRSA	35.80 ± 1.79	79.50 ± 3.56	84.80 ± 4.62

Moreover, approximately 49% of cell viability was reduced in 20 mg L^{-1} PA sample after 24 h.

Effects of PA and MAA (P-334) on photosynthetic pigments

Chlorophyll *a* The effect of 12 h incubation under 0, 2, 4 and 8 mg L^{-1} PA and PA + P-334 on photosynthetic pigments in *Anabaena* sp. HKAR-7 is shown in Fig. 9a. The results show varied Chl *a* concentration under exposed stress. The Chl *a* concentration reduced by 24% (0.94 µg mL^{-1}), 52% (0.57 µg mL^{-1}) and 68% (0.40 µg mL^{-1}) in 2, 4 and 8 mg L^{-1} PA treated samples respectively after 12 h. However, this decline was comparatively less i.e., 11% (1.2 µg mL^{-1}), 26% (0.90 µg mL^{-1}) and 53% (0.81 µg mL^{-1}) in 2, 4 and 8 mg L^{-1} PA + P-334 treated samples, respectively. Samples without PA and with P-334 had enhanced Chl *a* (1.35 µg mL^{-1}) and (1.42 µg mL^{-1}) as compared to control (1.23 µg mL^{-1}) after 12 h.

Carotenoids Carotenoids content increased by up to 183% (54.80 µg mL^{-1}) and 164% (50.78 µg mL^{-1}) in the 2 mg L^{-1} PA and PA + P-334 treated samples respectively after 12 h. Thereafter, a decrease was recorded with increased doses of PA and maximum decrease was 32% (23.28 µg mL^{-1}) in the 8 mg L^{-1} PA exposed samples. Carotenoid concentration was relatively high, i.e., 35.60 µg mL^{-1} (without PA treated sample) and 37.12 µg mL^{-1} (with P-334 treated samples) as compared to the control, i.e., 30.70 µg mL^{-1} after 12 h (Fig. 9b).

Phycocyanin (PC) The PC content was adversely affected by PA and declined by 29% (0.17 mg mL^{-1}), 60% (0.096 mg mL^{-1})

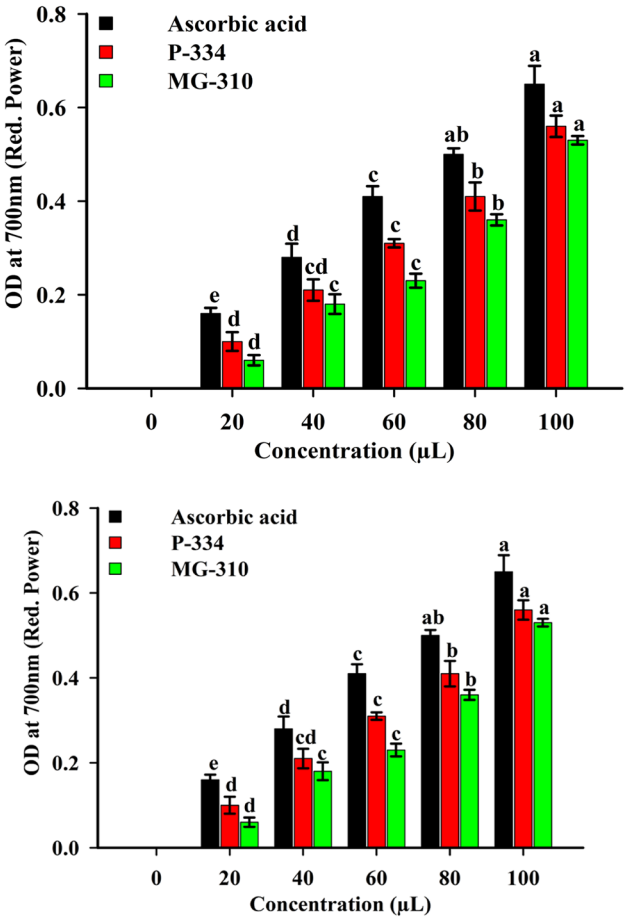

Fig. 6 Reducing potentials of porphyra-334 (P-334), mycosporine glycine-310 (MG-310) and ascorbic acid with their corresponding doses of 0, 20, 40, 60, 80 and 100 µL. The error bars denote standard deviations of means ($n=3$). Similar letters over bar represent homogeneous mean group ($P>0.05$)

and 73% (0.062 mg mL^{-1}) in 2, 4 and 8 mg L^{-1} in the 12 h PA exposed samples (Fig. 9c). Under PA + P-334 exposure it was 16% (0.21 mg mL^{-1}), 37% (0.15 mg mL^{-1}) and 54% (0.12 mg mL^{-1}) in 2, 4 and 8 mg L^{-1} PA exposed samples for 12 h.

Total protein

Total protein contents increased under 0 and 2 mg L^{-1}, PA and PA + P-334 treatment as compared to the control (0.40 mg mL^{-1}). Thereafter, a decrease of approximately 20% (0.33 mg mL^{-1}) and 42% (0.23 mg mL^{-1}) was observed in the 4 and 8 mg L^{-1} PA treated samples after 12 h (Fig. 9d).

Photosynthetic activity

Maximum photochemical efficiency (quantum yield) of open reaction centre (RC)IIs (F_v/F_m) and relative electron transport rate ($rETR_{max}$) of *Anabaena* sp. HKAR-7 were negatively affected by PA, whereas this effect was comparatively less in samples supplemented with exogenous P-334 along with PA (Table 4). The PA treatment causes considerable decrease in F_v/F_m by 22% (0.29), 50% (0.19) and 76% (0.09) upon 2, 4 and 8 mg L^{-1} PA exposure, respectively. Similarly, the decline in F_v/F_m was 13% (0.33), 26% (0.28) and 44% (0.21) upon 2, 4 and 8 mg L^{-1} PA + P-334 exposure, respectively. The $rETR_{max}$ value declined up to 32%, 53%, and 77% after 2, 4 and 8 mg L^{-1} PA treatment, respectively. The decline of $rETR_{max}$ percentage was comparatively less in samples treated with 2, 4 and 8 mg L^{-1} of PA + P-334.

Superoxide dismutase (SOD) and Catalase (CAT)

The SOD and CAT activities increased in all treated samples as compared to the control (Table 5). SOD activity increases up to 152% (0.32), 204% (0.43), 271% (0.57) in 2, 4 and 8 mg L^{-1} PA treatments and 123% (0.26), 147% (0.31), 195% (0.41) in 2, 4 and 8 mg L^{-1} PA + P-334 treatments. Similar trends were also recorded in CAT activity. CAT activity was comparatively less, i.e., 138% (0.38 U mol min^{-1} mg^{-1} protein), 168% (0.49 U mol min^{-1} mg^{-1} protein), 203% (0.59 U mol min^{-1} mg^{-1} protein) in 2, 4 and 8 mg L^{-1} PA + P-334 treatments.

Detection of intracellular ROS level

A significant amount of ROS was generated under different concentrations of PA and PA + P-334 in *Anabaena* sp. HKAR-7 (Fig. 10a) 0, 2, 4 and 8 mg L^{-1} PA had more pronounced visible changes after 12 h, whereas treatment with PA (0, 2, 4 and 8 mg L^{-1}) along with P-334 showed comparatively low fluorescence signals in the cell filaments. DCF and Chl *a* autofluorescence derived green and red ratio (G/R) was analyzed under 0, 2, 4 and 8 mg L^{-1} PA and PA + P-334 (Fig. 10b) that the G/R ratio increased with an increase in PA concentration in a dose-dependent manner. The G/R ratio was maximum i.e., 1.48 (495%) in 8 mg L^{-1} PA, whereas it was 0.90 (298%) in 8 mg L^{-1} PA + P-334 treated samples after 12 h (Fig. 10c).

The MAA was utilized as antioxidant to distinguish the ROS scavenging activity incited by H_2O_2. High doses of PA exposure results in enhanced ROS generation. The ROS generation reached up to 385% (345 AU) and 512% (470 AU) in 4 and 8 mg L^{-1} PA treated samples, respectively, as compared to the control (89 AU). Comparatively decreased DCF fluorescence level was recorded in samples exposed to 4 and 8 mg L^{-1} PA + P-334 and it was 263% (237 AU) and 325% (292 AU), respectively, after 12 h.

Lipid peroxidation, DNA strand breaks and gel electrophoresis

Figure 11a and b show PA-induced DNA strand breaks and lipid peroxidation with and without P-334 exposure in

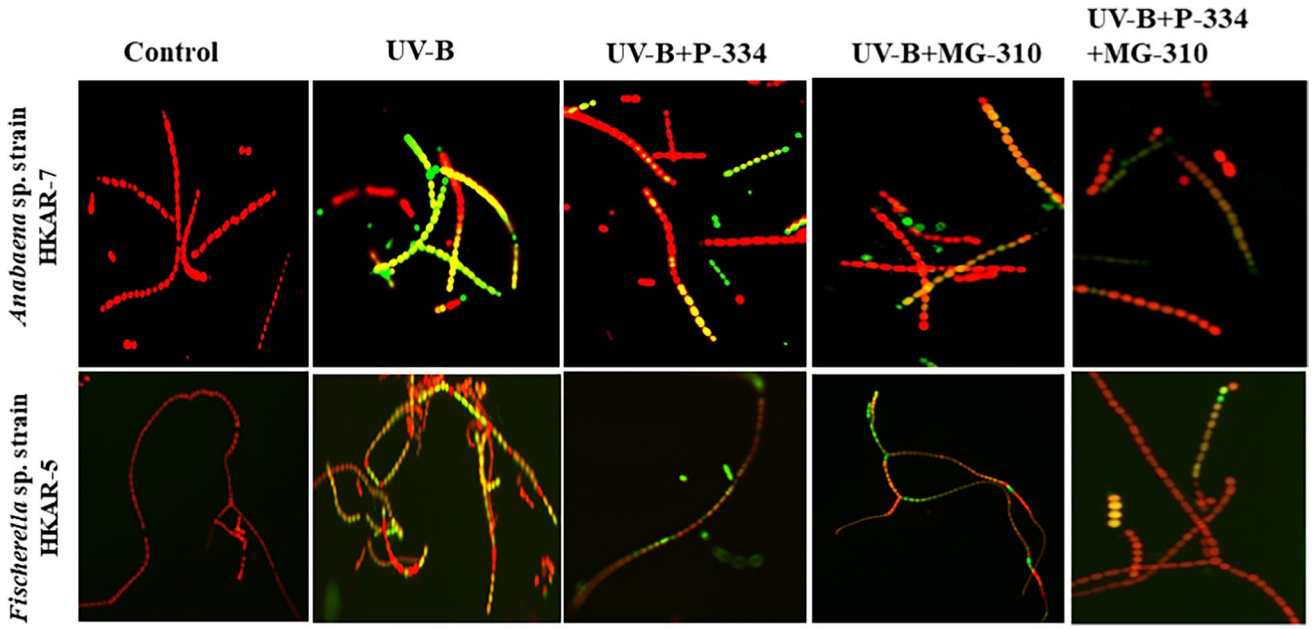

Fig. 7 Fluorescence images of *Anabaena* sp. HKAR-7 (**a**) and *Fischerella* sp. HKAR-5 (**b**) after 12 h exposure of UV-B, UV-B + porphyra-334 (P-334), UV-B + mycosporine glycine-310 (MG-310) and UV-B + P-334 + MG-310. Fluorescence images showing the generation of intracellular reactive oxygen species (ROS) (green DCF fluorescence)

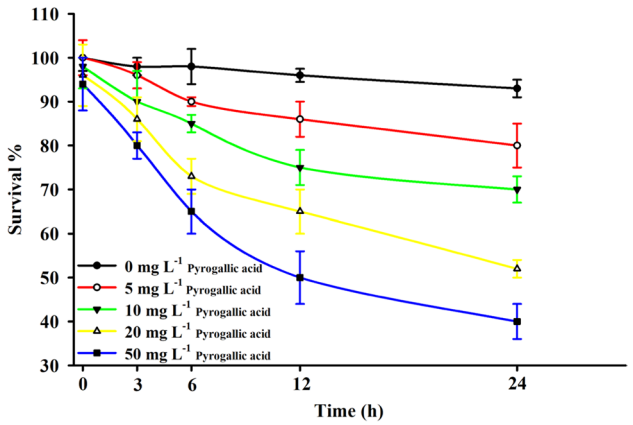

Fig. 8 Changes in percentage survival of *Anabaena* sp. HKAR-7 in response to different concentrations of pyrogallic acid (0, 5, 10, 20 and 50 mg L^{-1}) for different duration of time. The error bar represents standard deviation of mean ($n = 3$)

Anabaena sp. HKAR-7. As the concentration of PA increased, DNA strand breakage and lipid peroxidation increased as compared to the control. Lipid peroxidation increased up to 150% (0.19 µmol MDA g^{-1} dry wt), 240% (0.30 µmol MDA g^{-1} dry wt), 338% (0.44 µmol MDA g^{-1} dry wt), 425% (0.55 µmol MDA g^{-1} dry wt) in samples exposed to 0, 2, 4 and 8 mg L^{-1} PA, respectively. Lipid peroxidation in 0, 2, 4 and 8 mg L^{-1} PA along with P-334 treated samples were 133% (0.17 µmol MDA g^{-1} dry wt), 176% (0.22 µmol MDA g^{-1} dry wt), 228% (0.29 µmol MDA g^{-1} dry wt), 334% (0.40 µmol MDA g^{-1} dry wt), respectively, after 12 h. A decreased dsDNA content of 43 and 60% was recorded in the 4 and 8 mg L^{-1} PA treated samples, respectively. Exogenous supplements of P-334 along with PA retain the dsDNA content with some extent. A positive relationship was seen between lipid peroxidation and ROS generation with respect to doses of PA in *Anabaena* sp. HKAR-7. Intensity of genomic DNA bands that depict the toxicity of PA in *Anabaena* sp. HKAR-7 is shown in Fig. 11c.

Discussion

Cyanobacteria can survive in a wide range of harsh environments such as brightly lit habitats having high UV fluxes. The present investigation compares the MAAs profile in two cyanobacteria, *Anabaena* sp. HKAR-7 and *Fischerella* sp. HKAR-5, from diverse habitats such as rice field and rock. The role of MAAs as antioxidants, their ROS scavenging and reducing potential were also investigated. Based on UV–Vis absorption spectra, HPLC and ESI–MS data, the single MAA, P-334 was tentatively identified from *Anabaena* sp. HKAR-7. However, three MAAs, shinorine, MG-310 and palythinol were identified in *Fischerella* sp. HKAR-5. Occurrence and composition of MAAs may vary within or among species (Sonntag et al. 2007). Similarily in our finding the cyanobacterium inhabiting rocks (*Fischerella* sp. HKAR-5) produced more diverse forms of MAAs (Shinorine, MG-310 and Palythinol) as compared to the rice-field cyanobacterium *Anabaena* sp. HKAR-7

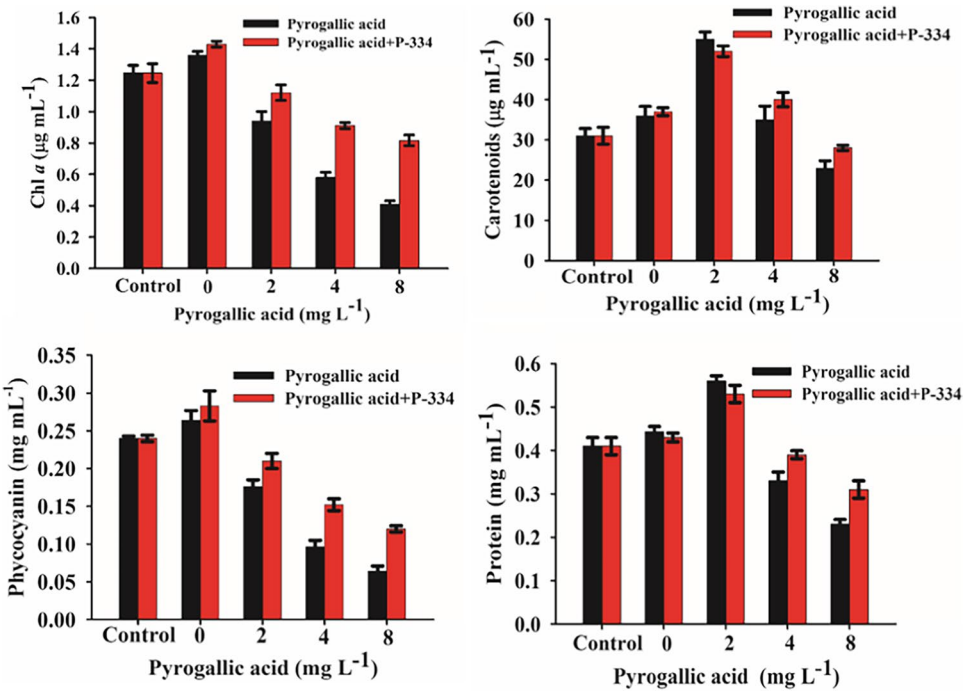

Fig. 9 Effects of pyrogallic acid with/without MAA, porphyra 334 (P-334) on Chl *a* (**a**) carotenoids (**b**) phycocyanin (**c**) and total protein content (**d**) in *Anabaena* sp. HKAR-7. Results are expressed as means of three replicates. Vertical bars indicate standard deviation of the means ($n=3$)

Table 4 Effects of different concentrations of PA with/without exposure of MAA, P-334 on maximum quantum yield (*Fv/Fm*) and maximum ETR in *Anabaena* sp. strain HKAR-7. Values represent means ± S.D ($n=3$)

Pyrogallic acid (mg L^{-1})	F_v/F_m		$rETR_{max}$	
	Pyrogallic acid	Pyrogallic acid + P-334	Pyrogallic acid	Pyrogallic acid + P-334
Control	0.38 ± 0.022	0.38 ± 0.020	92 ± 8.0	92 ± 6.90
0	0.39 ± 0.03	0.41 ± 0.01	96 ± 4.2	98 ± 9.30
2	0.29 ± 0.019	0.33 ± 0.019	62 ± 5.3	77 ± 7.20
4	0.19 ± 0.028	0.28 ± 0.018	43 ± 6.1	68 ± 5.80
8	0.09 ± 0.011	0.21 ± 0.012	21 ± 3.1	39 ± 2.20

Table 5 Effect of different concentration of PA with/without exposure of MAA, P-334 on SOD and catalase activity in *Anabaena* sp. strain HKAR-7. Values represent means ± S.D, ($n=3$)

Pyrogallic acid (mg L^{-1})	SOD (U mg^{-1} protein)		CAT (μmol min^{-1} mg^{-1} protein)	
	Pyrogallic acid	Pyrogallic acid + P-334	Pyrogallic acid	Pyrogallic acid + P-334
Control	0.21 ± 0.02	0.21 ± 0.03	0.29 ± 0.03	0.29 ± 0.02
0	0.23 ± 0.04	0.17 ± 0.01	0.32 ± 0.02	0.25 ± 0.01
2	0.32 ± 0.03	0.26 ± 0.02	0.54 ± 0.03	0.38 ± 0.02
4	0.43 ± 0.02	0.31 ± 0.03	0.67 ± 0.05	0.49 ± 0.04
8	0.57 ± 0.03	0.41 ± 0.02	0.86 ± 0.02	0.59 ± 0.06

(Single MAA, P-334), explain its role in survial of cyanobacterium. Possibly, *Fischerella* sp. HKAR-5 growing on rocks face various abiotic stresses including desiccation and UV-B radiation and this could be the reason for the synthesis of diverse forms of MAAs in this cyanobacterium. In cyanobacteria, MAAs can bind to their cell wall (Ehling-Schulz et al. 1997) or can be distributed homogeneously within the cytoplasm (Garcia-Pichel and Castenholz 1993). As effective photoprotectants, MAAs provide broad band UV filtration to several terrestrial and aquatic organisms. It was found that MAAs prevent three out of ten photons from hitting the cytoplasmic targets and high concentrations of MAAs in cells provide approximately 25% more resistance to UVR (Garcia-Pichel et al. 1993). The presence of a

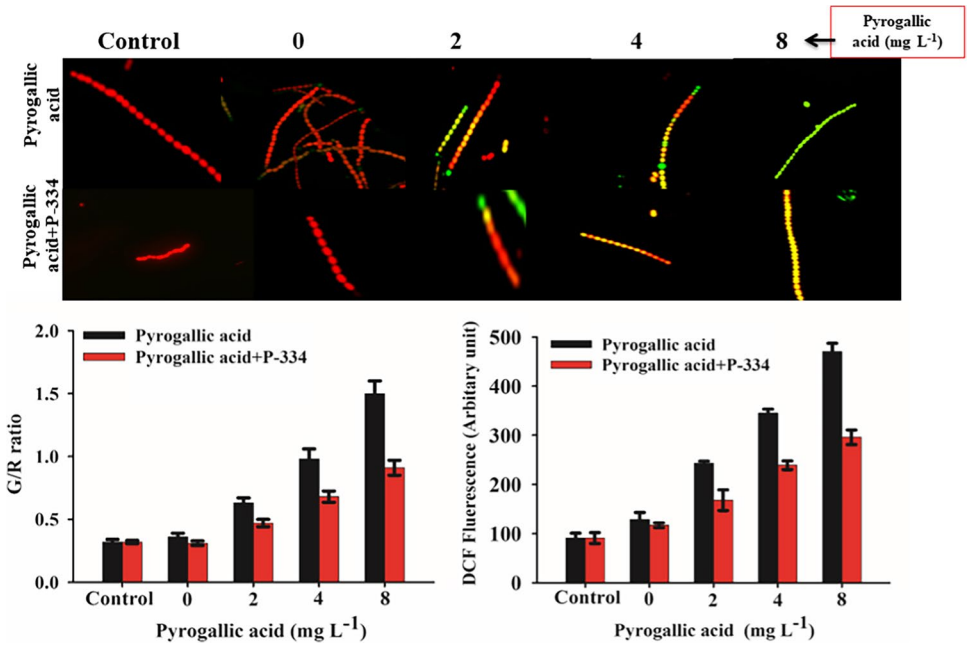

Fig. 10 Fluorescence images (**a**), fluorescence-based Green/Red (G/R) ratio (**b**), reactive oxygen species (ROS) generation (**c**) under different doses of pyrogallic acid along with or without MAA (porphyra-334; P-334) in *Anabaena* sp. HKAR-7. Vertical bars indicate the standard deviation of the means ($n = 3$)

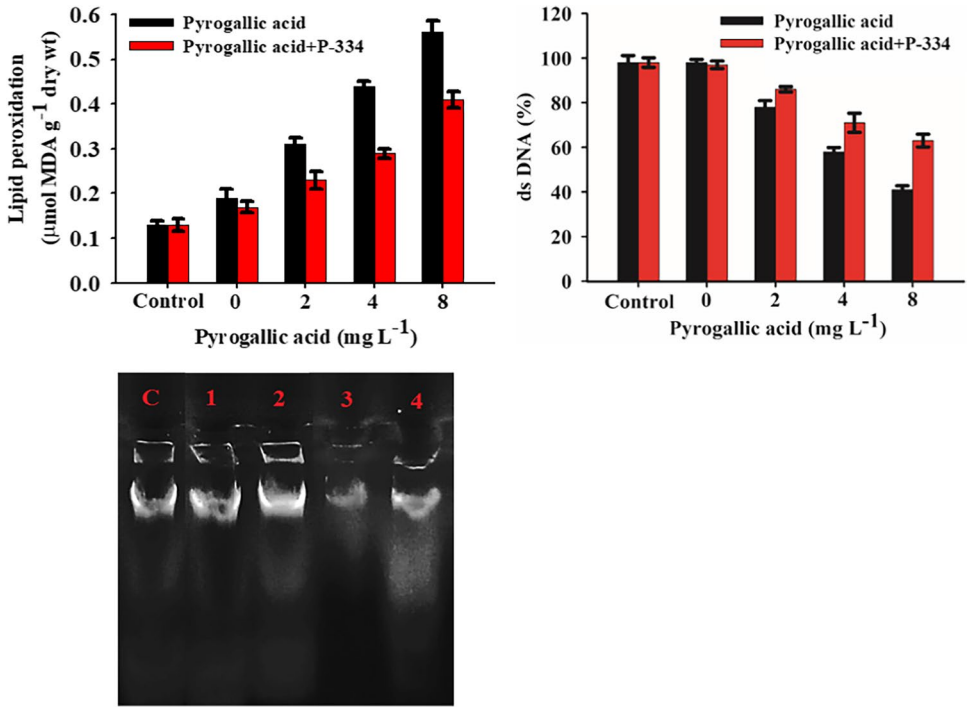

Fig. 11 Effect of pyrogallic acid (PA) and PA + porphyra 334 (P-334) on lipid peroxidation (**a**) ds DNA break (**b**) genomic DNA banding pattern (**c**) in *Anabaena* sp. HKAR-7 after 12 h. Vertical bars indicate standard deviation of the means. ($n = 3$) C: Control; 1: 4 mg L^{-1} PA; 2: 4 mg L^{-1} PA + P-334; 3: 8 mg L^{-1} PA; 4: 8 mg L^{-1} PA + P-334

higher concentration of MAAs in cyanobacteria highlights their role in stress management. Our results also support the inductive role of UV-B radiation on MAAs biosynthesis. Besides, exposure of PAR + UV-A + UV-B radiation has a more effective role in MAAs synthesis in both the studied cyanobacteria.

MG and the precursor of MAAs, gadusol act as antioxidants and prevent cellular damage occuring from ROS which are generated upon UVR exposure (Coba et al. 2009). Moreover, accumulation or biosynthesis of photoprotective compounds such as MAAs protects the cellular organelles from the deleterious impacts of UVR (Singh et al. 2010, 2022). The MAA P-334 is commonly found in the red alga *Porphyra* as well as in a number of cyanobacteria. However, information regarding its detailed chemical characterization is scarce and its exogenous application against strong allelochemicals such as PA has been performed for the first time. The presence of P-334, shinorine and MG-310

has been documented in different genera of cyanobacteria (Garcia-Pichel and Castenholz 1993; Sinha et al. 2001a, b; Torres et al. 2006; Singh et al. 2008a, b, 2010; Khanipour et al. 2015). In contrast to other MAAs, the presence of palythinol is reported for the first time in *Fischerella* sp. inhabiting rock habitats.

Photoprotection, physicochemical stability, wide distribution and diversity of MAAs make them an unique group of sun-screening compounds (Rastogi et al. 2016). Similarily, we observed that, two MAAs (P-334 and MG-310) were efficient stable metabolites that showed strong resistivity against different physicochemical stressors, such as temperature, UV-B, strong oxidizing agent (H_2O_2) and pH. Apart from the important role as sunscreen agents, MAAs also play role in several biological processes of organisms (Mason et al. 1998; Neale et al. 1998; Bandaranayake and Des Rocher 1999; Shick and Dunlap 2002; Oren and Gunde-Cimerman 2007) and their embryos (Adams and Shick 2001), such as osmotic regulation (Oren 1997; Portwich and Garcia-Pichel 1999; Sinha and Häder 2003; Kogej et al. 2006; Singh et al. 2008a, b; Waditee-Sirisattha et al. 2014), antioxidant and ROS scavenging properties (Rastogi et al. 2016), defense against oxidative and thermal stresses (Michalek-Wagner 2001; Shick and Dunlap 2002), and desiccation tolerance (Feng et al. 2012; Olsson-Francis et al. 2013). On the basis of photophysical and photochemical studies, it was found that MAAs absorb UVR and release it almost completely as heat, without the generation of ROS (Conde et al. 2000, 2004). MAAs help in maintaining the antioxidant defense system of the skin, similar to the expression of Hsp70 through its antioxidant activity (Coba et al. 2007a, b, 2009). Similarily in our study, the different antioxidant assays also showed that the studied MAAs, P-334 and MG-310, acted as strong antioxidants that quench ROS inside the cells. MAAs also decreased ROS generation as confirmed by in vitro incubation of both MAAs separately as well with their combination as also supported by fluorescence images of in vitro incubated cyanobacterial samples. Thus it can be concluded that MAAs are efficient and stable sunscreen compounds that act as strong antioxidants and ROS quenchers. It has been found that allelopathic compounds influence several life processes in phytoplankton, for example, cell division, photosynthesis, enzyme activity, water and minerals uptake, and signal transduction (Belz and Hurle 2004; Hong et al. 2009; Inderjit and Duke 2003).

PA is used commonly in many industrial and consumer products and is widely distributed in nature (Upadhyay et al. 2010; Avase et al. 2015). Despite its beneficial properties, PA-mediated toxicity has been a major concern. It has been reported that PA showed mutagenic effects and liver, lung, kidney and gastrointestinal tract were its major target organs (Upadhyay et al. 2010). Recently, PA as a strong allelochemical attracted attention. Release of the allelochemicals (secondary metabolite) by the submerged macrophytes is considered to be a way to inhibit the growth of phytoplankton (Gross 2003; Hilt and Gross 2008). As discussed previously, it was found that the inhibitory effect of PA against *M. aeruginosa* may involve oxidative stress (Wu et al. 2007), photosynthesis inhibition (Dziga et al. 2007; Zhu et al. 2010; Wu et al. 2013) and interfering the expression of antioxidative gene (Shao et al. 2009). Studies showed that DNA strands and the cell membrane were two targets of ROS induced by PA, and oxidative damage was an important mechanism for the toxicity of PA against *M. aeruginosa* (Lu et al. 2016). It might be possible that in natural conditions cyanobacteria protect themselves from the allelopathic effect of PA by synthesizing MAAs. The present study gives an insight about the possible role of P-334 as a defense strategy against PA in cyanobacteria. It also explores the allelopathy mechanism of PA in terms of lipid peroxidation (MDA formation) and denaturation of dsDNA (DNA bands) that may be helpful for controlling the harmful bloom forming cyanobacteria population and water quality deterioration. This allelopathy mechanism of action provides great promise for treating harmful algal blooms.

We also tried to assess the antioxidant and metabolic responses of *Anabaena* sp. HKAR-7 to PA, and exogenous supplement of P-334 in terms of photosynthetic pigments, photosynthetic efficiency, ROS generation, antioxidative enzymes, lipid peroxidation and DNA damage. Our observations revealed that higher doses (20 and 50 mg L^{-1}) of PA exposure strongly inhibited survival of this cyanobacterium with increased exposure time. Wu et al. (2013) also found that 4 mg L^{-1} of PA significantly inhibited the growth of the cyanobacterium *Cylindrospermopsis raciborskii* F2. Similarly, photosynthetic pigments such as Chl *a* and PC content were adversely influenced under different doses of PA. Samples exposed to PA along with P-334 showed fewer damaging effects in comparison to those treated by PA alone. PC was found to more sensitive in comparison to Chl *a* under high doses (4 and 8 mg L^{-1}) of PA.

Carotenoids and total cellular protein content increased under low doses of PA (2 mg L^{-1}), whereas increased doses of PA (4 and 8 mg L^{-1}) caused detrimental effects. It is possible that higher doses of PA exposure led to enhanced cellular ROS generation and membrane disintegration subsequently leading to impairment of photosynthetic pigments and protein content. It might be possible that PA-induced generation of ROS is reduced exogenous supplement of P-334. Photosynthetic inhibition and oxidative harm were seen as significant methods of action for the allelopathic impact of PA on *C. raciborskii* F2 (Wu et al. 2013). In our findings, the photosynthetic inducators, F_v/F_m and $rETR_{max}$ also were affected adversely in all PA treatments.

PA exposure induces enhanced ROS generation in cyanobacteria which triggers the enzymatic antioxidant defense system increasing SOD and CAT activities (Wu et al. 2013). We also observes the existence of antioxidative responses (SOD and CAT activities) in *Anabaena* sp. HKAR-7 after PA exposure in a dose-dependent manner. However,

PA + P-334 treated samples showed comparably less SOD and CAT activity. Therefore, it can be concluded that P-334 played a role in the reduction of PA-induced generated ROS.

We attempted to recognize the extent of ROS level in vivo by utilizing an oxidant-detecting probe DCFH-DA. In our study, cyanobacterial filaments were found to change their color from red to green as the intracellular ROS generation increased due to PA exposure. This shift was comparatively less in PA + P-334 exposed samples as also indicated by the G/R ratio Wu et al (2013) similarly found that high doses of PA repressed the growth of *C. raciborskii* F2 and brought about a change in the oxidative system and the expression of seven key genes (Wu et al. 2013).

In the present investigation, DNA strand breaks were enhanced as the dose of PA increased. Similar patterns were also seen in lipid peroxidation in *Anabaena* sp. HKAR-7 as shown by MDA values. Therefore, it can be concluded that extensive ROS formation causes lipid peroxidation (MDA formation) and denaturation of dsDNA (DNA bands). PA together with exogenous P-334 reduces the detrimental effects caused by ROS, therefore, MDA formation and unwinding percentage of dsDNA was comparatively low. This explains the crucial role of P-334 as antioxidant against cellular ROS under stressed conditions.

Supplementary Information The online version contains supplementary material available at https://doi.org/10.1007/s10811-022-02832-w.

Acknowledgements Authors are also thankful to the Interdisciplinary School of Life Sciences (ISLS), BHU, Varanasi, India, for providing access to the ESI-MS and fluorescence microscopy facility. Department of Chemistry, BHU, Varanasi, India, is acknowledged for providing FTIR and NMR facilities.

Authors' contributions Deepak K. Singh, designed and conducted the experiments, analyzed the data and wrote the manuscript. Jainendra Pathak helped in data analyses, writing and editing the manuscript. Abha Pandey, Vidya Singh, and Rajneesh helped in performing the experiments. Rajeshwar P. Sinha provided laboratory facilities and edited the manuscript. The final manuscript was read and approved by all the authors.

Funding Deepak K. Singh (09/013(0612)/2015-EMR-I), Jainendra Pathak (09/013/0515/2013-EMR-I), Abha Pandey (09/013/0619/2016-EMR-I), and Vidya Singh (09/013(0568)/2014-EMR-I) are thankful to Council of Scientific and Industrial Research, New Delhi, India, for the financial support in the form of senior research fellowships. Rajneesh is grateful to the Department of Biotechnology, Govt. of India, (DBT-JRF/13/AL/143/2158), for the grant in the form of senior research fellowship.

Data availability The data can be obtained from the corresponding author on reasonable request.

Declarations

Conflicts of interest The authors declare no conflict of interest.

References

Adams NL, Shick JM (2001) Mycosporine-like amino acids prevent UV-B induced abnormalities during early development of the green sea urchin *Strongylocentrotus droebachiensis*. Mar Biol 138:267–280

Ahmed H, Pathak J, Rajneesh, Sonkar PK, Ganesan V, Häder D-P, Sinha RP (2021a) Responses of a hot spring cyanobacterium under ultraviolet and photosynthetically active radiation: photosynthetic performance, antioxidative enzymes, mycosporine-like amino acid profiling and its antioxidative potentials. 3 Biotech 11:1–23

Ahmed H, Pathak J, Singh DK, Pandey A, Rajneesh SV, Kumar D, Singh PR, Sinha RP (2021b) Phytoplankton assemblage and UV-protective compounds in the river Ganges. Indian J Tradit Knowl 20:191–203

Avase SA, Srivastava S, Vishal K, Ashok HV, Varghese G (2015) Effect of pyrogallol as an antioxidant on the performance and emission characteristics of biodiesel derived from waste cooking oil. Proc Earth Planet Sci 11:437–444

Bandaranayake WM, Des Rocher A (1999) Role of secondary metabolites and pigments in the epidermal tissues, ripe ovaries, viscera, gut contents and diet of the sea cucumber *Holothuria atra*. Mar Biol 133:163–169

Belz RG, Hurle K (2004) A novel laboratory screening bioassay for crop seeding allelopathy. J Chem Ecol 30:175–198

Bradford MM (1976) A rapid and sensitive method for the quantification of microgram quantity of proteins utilizing the principle of protein dye binding. Anal Biochem 72:248–254

Bryant DA, Guglielmi G, Tandeau de Marsac N, Castlets AM, Cohen-Bazire G (1979) The structure of cyanobacterial phycobilisomes: a model. Arch Microbiol 123:113–127

Burja AM, Dhamwichukorn S, Wright PC (2003) Cyanobacterial postgenomic research and systems biology. Trends Biotechnol 21:504–511

Chen LZ, Wang GH, Hong S, Liu A, Liu YD (2009) UV-B-induced oxidative damage and protective role of exopolysaccharides in desert cyanobacterium, *Microcoleus vaginatus*. J Integr Plant Biol 51:194–200

Coba FDL, Aguilera J, Figueroa FL (2007a) Use of mycosporine-type amino acid shinorine as an antioxidant. International Patent WO2007a/026038A2

Coba FDL, Aguilera J, Figueroa FL (2007b) Use of mycosporine-type amino acid Porphyra-334 as an antioxidant. International Patent WO2007b/026035A2

Coba FDL, Aguilera J, Figueroa FL, de Gálvez MV, Herrera E (2009) Antioxidant activity of mycosporine-like amino acids isolated from three red macroalgae and one marine lichen. J Appl Phycol 21:161–169

Codd GA, Lindsay J, Young FM, Morrison LF, Metcalf JS (2005) Harmful cyanobacteria. In: Huisman J, Matthijs HCP, Visser PM (eds) Harmful cyanobacteria. Springer, Dordrecht pp 1–23

Conde FR, Churio MS, Previtali CM (2000) The photoprotector mechanism of mycosporine-like amino acids. Excited-state properties and photostability of porphyra-334 in aqueous solution. J Photochem Photobiol B 56:139–144

Conde FR, Churio MS, Previtali CM (2004) The deactivation pathways of the excited-states of the mycosporine-like amino acids shinorine and porphyra-334 in aqueous solution. Photochem Photobiol Sci 3:960–967

Cosgrove J, Borowitzka MA (2011) Chlorophyll fluorescence terminology: An introduction. In: Suggett DJ, Prásil O, Borowitzka MA (eds) Chlorophyll *a* fluorescence in aquatic sciences: methods and applications. Springer, Dordrecht, pp 1–17

Crutzen PJ (1992) Ultraviolet on the increase. Nature 356:104–105

Donahue JL, Okpodu CM, Cramer CL, Grabau EA, Alscher RG (1997) Responses of antioxidants to paraquat in pea leaves (relationships to resistance). Plant Physiol 113:249–257

Dunn WB, Bailey NJC, Johnson HE (2005) Measuring the metabolome: current analytical technologies. Analyst 130:606–625

Dziga D, Suda M, Bialczyk J, Urszula CP, Lechowski Z (2007) The alteration of *Microcystis aeruginosa* biomass and dissolved microcystin-LR concentration following exposure to plant-producing phenols. Environ Toxicol 22:341–346

Ehling-Schulz M, Bilger W, Scherer S (1997) UV-B-induced synthesis of photoprotective pigments and extracellular polysaccharides in the terrestrial cyanobacterium *Nostoc commune*. J Bacteriol 179:1940–1945

Feng YN, Zhang ZC, Feng JL, Qiu BS (2012) Effects of UV-B radiation and periodic desiccation on the morphogenesis of the edible terrestrial cyanobacterium *Nostoc flagelliforme*. Appl Environ Microbiol 78:7075–7081

Fischer WF (2008) Life before the rise of oxygen. Nature 455:1051–1052

Gao K, Wu Y, Li G, Wu H, Villafañe VE, Helbling EW (2007a) Solar UV radiation drives CO_2 fixation in marine phytoplankton: A double-edged sword. Plant Physiol 144:54–59

Gao K, Yu H, Brown MT (2007b) Solar PAR and UV radiation affects the physiology and morphology of the cyanobacterium *Anabaena* sp. PCC 7120. J Photochem Photobiol B 89:117–124

Garcia-Pichel F, Castenholz RW (1993) Occurrence of UV-absorbing, mycosporine-like compounds among cyanobacterial isolates and an estimate of their screening capacity. Appl Environ Microbiol 59:163–169

García-Pichel F, Wingard CE, Castenholz RW (1993) Evidence regarding the UV sunscreen role of a mycosporine-like compound in the cyanobacterium *Gloeocapsa* sp. Appl Environ Microbiol 59:170–176

Genty B, Briantais JM, Baker NR (1989) The relationship between the quantum yield of photosynthesis electron transport and quenching of chlorophyll fluorescence. Biochem Biophys Acta 990:87–92

Gross EM (2003) Allelopathy of aquatic autotrophs. Crit Rev Plant Sci 22:313–339

Gross EM, Meyer H, Schilling G (1996) Release and ecological impact of algicidal hydrolysable polyphenols in *Myriophyllum spicatum*. Phytochemistry 41:133–138

Häder D-P, Kumar HD, Smith RC, Worrest RC (2007) Effects of solar UV radiation on aquatic ecosystems and interactions with climate change. Photochem Photobiol Sci 6:267–285

He YY, Häder D-P (2002a) Reactive oxygen species and UV-B: effect on cyanobacteria. Photochem Photobiol Sci 1:729–736

He YY, Häder D-P (2002b) UV-B-induced formation of reactive oxygen species and oxidative damage of the cyanobacterium *Anabaena* sp.: protective effects of ascorbic acid and N-acetyl-L-cysteine. J Photochem Photobiol B 66:115–124

Hilt S, Gross EM (2008) Can allelopathically active submerged macrophytes stabilise clear-water states in shallow lakes? Basic Appl Ecol 9:422–443

Hong Y, Hu H, Xie X, Sakoda A, Sagehashi M, Li F (2009) Gramine-induced growth inhibition, oxidative damage and antioxidant responses in freshwater cyanobacterium *Microcystis aeruginosa*. Aquat Toxicol 91:262–269

Hu C, Völler G, Süßmuth R, Dittmann E, Kehr JC (2015) Functional assessment of mycosporine-like amino acids in *Microcystis aeruginosa* strain PCC 7806. Environ Microbiol Rep 17:1548–1559

Inderjit, Duke SO (2003) Ecophysiological aspects of allelopathy. Planta 217:529–539

Jain S, Prajapat G, Abrar M, Ledwani L, Singh A, Agrawal A (2017) Cyanobacteria as efficient producers of mycosporine-like amino acids. J Basic Microbiol 57:715–727

Jantaro S, Pothipongsa A, Khanthasuwan S, Incharoensakdi A (2011) Short-term UV-B and UV-C radiations preferentially decrease spermidine contents and arginine decarboxylase transcript levels of *Synechocystis* sp. PCC 6803. Curr Microbiol 62:420–426

Jensen A (1978) Chlorophylls and carotenoids. In: Hellebust JA, Craige IS (eds) Handbook of phycological methods: physiological and biochemical methods. Cambridge University Press, Cambridge, pp 59–70

Kannaujiya VK, Sinha RP (2015) Impacts of varying light regimes on phycobiliproteins of *Nostoc* sp. HKAR-2 and *Nostoc* sp. HKAR-11 isolated from diverse habitats. Protoplasma 252:1551–1561

Karentz S, Cleaver JE, Mitchell DL (1991) DNA damage in the Antarctic. Nature 350:28

Khanipour RS, Farhangi M, Emtyazjoo M, Rabbani M (2015) Effects of solar radiation on pigmentation and induction of a mycosporine-like amino acid in two cyanobacteria, *Anabaena* sp. and *Nostoc* sp. ISC26. Eur J Phycol 50:173–181

Kogej T, Gostinčar C, Volkmann M, Gorbushina AA (2006) Mycosporines in extremophilic fungi-novel complementary osmolytes? Environ Chem 3:105–110

Kulisic T, Radonic A, Katalinic V, Milos M (2004) Use of different methods for testing antioxidative activity of oregano essential oil. Food Chem 85:633–640

Kumar D, Kannaujiya VK, Jaiswal J, Sinha RP (2020) Effects of ultraviolet and photosynthetically active radiation on phycocyanin of habitat specific cyanobacteria. J Sci Res 64:74–79

Lesser MP (2008) Effects of ultraviolet radiation on productivity and nitrogen fixation in the cyanobacterium, *Anabaena* sp. (Newton's strain). Hydrobiologia 598:1–9

Leu E, Krieger-Liszkay A, Goussias C, Gross EM (2002) Polyphenolic allelochemicals from the aquatic angiosperm *Myriophyllum spicatum* inhibit photosystem II. Plant Physiol 130:2011–2018

Li X (2012) Improved pyrogallol autoxidation method: a reliable and cheap superoxide-scavenging assay suitable for all antioxidants. J Agric Food Chem 60:6418–6424

Lu Z, Zhang Y, Gao Y, Liu B, Sun X, He F, Zhou Q, Wu Z (2016) Effects of pyrogallic acid on *Microcystis aeruginosa*: oxidative stress related toxicity. Ecotoxicol Environ Saf 132:413–419

Manney GL, Santee ML, Rex M, Livesey NJ, Pitts MC, Veefkind P, Nash ER, Wohltmann I, Lehmann R, Froidevaux L, Poole LR, Schoeberl MR, Haffner DP, Davies J, Dorokhov V, Gernandt H, Johnson B, Kivi R, Kyrö E, Larsen N, Levelt PF, Makshtas A, McElroy CT, Nakajima H, Parrondo MC, Tarasick DW, von der Gathen P, Walker KA, Zinoviev NS (2011) Unprecedented Arctic ozone loss in 2011. Nature 478:469–475

Mason DS, Schafer F, Shick JM, Dunlap WC (1998) Ultraviolet radiation absorbing mycosporine-like amino acids (MAAs) are acquired from their diet by medaka fish (*Oryzias latipes*) but not by SKH-1 hairless mice. Comp Biochem Physiol A 120:587–598

Matsui K, Nazifi E, Kunita S, Wada N, Matsugo S, Sakamoto T (2011) Novel glycosylated mycosporine-like amino acids with radical scavenging activity from the cyanobacterium *Nostoc commune*. J Photochem Photobiol B 105:81–89

Mayer AM, Clifford JA, Aldulescu M, Frenkel JA, Holland MA, Hall ML, Glaser KB, Berry J (2011) Cyanobacterial *Microcystis aeruginosa* lipopolysaccharide elicits release of superoxide anion, thromboxane B_2, cytokines, chemokines, and matrix metalloproteinase-9 by rat microglia. Toxicol Sci 121:63–72

Melzer A (1999) Aquatic macrophytes as tools for lake management. In: Harper DM, Brierley B, Ferguson AJD, Phillips G (eds) The Ecological Bases for Lake and Reservoir Management. Springer, Dordrecht, pp 181–190

Michalek-Wagner K (2001) Seasonal and sex-specific variations in levels of photoprotecting mycosporine-like amino acids (MAAs) in soft corals. Mar Biol 139:651–660

Nakai S, Inoue Y, Hosomi M, Murakami A (2000) *Myriophyllum spicatum*-released allelopathic polyphenols inhibiting growth of blue-green algae *Microcystis aeruginosa*. Water Res 34:3026–3032

Neale PJ, Banaszak AT, Jarriel CR (1998) Ultraviolet sunscreens in *Gymnodinium sanguineum* (Dinophyceae): mycosporine-like amino acids protect against inhibition of photosynthesis. J Phycol 34:928–938

Olsson-Francis K, Watson JS, Cockell CS (2013) Cyanobacteria isolated from the high-intertidal zone: a model for studying the physiological prerequisites for survival in low Earth orbit. Int J Astrobiol 12:292–303

Oren A (1997) Mycosporine-like amino acids as osmotic solutes in a community of halophilic cyanobacteria. Geomicrobiol J 14:231–240

Oren A, Gunde-Cimerman N (2007) Mycosporines and mycosporine-like amino acids: UV protectants or multipurpose secondary metabolites? FEMS Microbiol Lett 269:1–10

Oyaizu M (1986) Studies on products of browning reaction. J Acad Nutr Diet 44:307–315

Oyamada C, Kaneniwa M, Ebitani K, Murata M (2008) Mycosporine-like amino acids extracted from scallop (*Patinopecten yessoensis*) ovaries: UV protection and growth stimulation activities on human cells. Mar Biotechnol 10:141–150

Pandey A, Pandey S, Rajneesh PJ, Ahmed H, Singh SP, Sinha RP (2017) Mycosporine-like amino acids (MAAs) profile of two marine red macroalgae *Gelidium* sp. and *Ceramium* sp. Int J Appl Sci Biotechnol 5:12–21

Pandey A, Pathak J, Singh DK, Ahmed H, Singh V, Kumar D (2020) Photoprotective role of UV-screening pigment scytonemin against UV-B-induced damages in the heterocyst-forming cyanobacterium *Nostoc* sp. strain HKAR-2. Braz J Bot 43:67–80

Pathak J, Rajneesh AH, Richa SRP (2017) Metabolomic profiling of cyanobacterial UV-protective compounds. Curr Metabolomics 5:138–163

Pathak J, Rajneesh MP, Singh SP, Häder D-P, Sinha RP (2018) Cyanobacterial farming for environment friendly sustainable agriculture practices: innovations and perspectives. Front Environ Sci 6:7

Pathak J, Singh PR, Häder D-P, Sinha RP (2019) UV-induced DNA damage and repair: A cyanobacterial perspective. Plant Gene 19:100194

Pathak J, Pandey A, Maurya PK, Rajneesh SRP, Singh SP (2020) Cyanobacterial secondary metabolite scytonemin: a potential photoprotective and pharmaceutical compound. Proc Nat Acad SciIndia B 90:467–481

Pathak J, Singh PR, Sinha RP, Rastogi RP (2021) Evolution and distribution of cyanobacteria. In: Rastogi RP (ed) Ecophysiology and biochemistry of cyanobacteria. Springer, Singapore, pp 1–30

Porra RJ (2002) The chequered history of the development and use of simultaneous equations for the accurate determination of chlorophylls *a* and *b*. Photosynth Res 73:149–156

Portwich A, Garcia-Pichel F (1999) Ultraviolet and osmotic stresses induce and regulate the synthesis of mycosporines in the cyanobacterium *Chlorogloeopsis* PCC 6912. Arch Microbiol 172:187–192

Rajneesh SSP, Pathak J, Sinha RP (2017a) Cyanobacterial factories for the production of green energy and value-added products: an integrated approach for economic viability. Renew Sustain Energy Rev 69:578–596

Rajneesh, Chatterjee A, Singh SP, Sinha RP (2017b) Detection of reactive oxygen species (ROS) in cyanobacteria using the oxidant-sensing probe 2,7'-dichlorodihydrofluorescein diacetate (DCFH-DA). Bio-protocol 7:2545

Rajneesh PJ, Häder D-P, Sinha RP (2019) Impacts of ultraviolet radiation on certain physiological and biochemical processes in cyanobacteria inhabiting diverse habitats. Environ Exp Bot 161:375–387

Rao MV, Paliyath G, Ormrod DP (1996) Ultraviolet-B and ozone induced biochemical changes in antioxidant enzymes of *Arabidopsis thaliana*. Plant Physiol 110:125–136

Rastogi RP, Sinha RP (2009) Biotechnological and industrial significance of cyanobacterial secondary metabolites. Biotechnol Adv 27:521–539

Rastogi RP, Singh SP, Häder D-P, Sinha RP (2010) Detection of reactive oxygen species (ROS) by the oxidant sensing probe 2',7'-dichlorodihydrofluorescein diacetate in the cyanobacterium *Anabaena variabilis* PCC 7937. Biochem Biophys Res Commun 397:603–607

Rastogi RP, Incharoensakdi A (2013) UV radiation-induced accumulation of photoprotective compounds in the green alga *Tetraspora* sp. CU2551. Plant Physiol Biochem 70:7–13

Rastogi RP, Incharoensakdi A (2014) Characterization of UV-screening compounds, mycosporine-like amino acids, and scytonemin in the cyanobacterium *Lyngbya* sp. CU2555. FEMS Microbiol Ecol 87:244–256

Rastogi RP, Singh SP, Incharoensakdi A, Häder DP, Sinha RP (2014) Ultraviolet radiation-induced generation of reactive oxygen species, DNA damage and induction of UV-absorbing compounds in the cyanobacterium *Rivularia* sp. HKAR-4. S Afr J Bot 90:163–169

Rastogi RP, Sonani RR, Madamwar D, Incharoensakdi A (2016) Characterization and antioxidant functions of mycosporine-like amino acids in the cyanobacterium *Nostoc* sp. R76DM. Algal Res 16:110–118

Richa RRP, Kumari S, Singh KL, Kannaujiya VK, Singh G, Kesheri M, Sinha RP (2011) Biotechnological potential of mycosporine-like amino acids and phycobiliproteins of cyanobacterial origin. Biotechnol Bioinform Bioeng 1:159–171

Richa, Sinha RP (2015) Biochemical characterization of sunscreening mycosporine-like amino acids from two *Nostoc* species inhabiting diverse habitats. Protoplasma 252:199–208

Richa, Sinha RP, Häder D-P (2016) Effects of global change, including UV and UV-screening compounds. In: Borowitzka MA, Beardall J, Raven JA (eds) The physiology of microalgae. Developments in applied phycology. Springer , Cham pp 373–409

Rippka R, Deruelles J, Waterbury JB, Herdman M, Stanier RY (1979) Generic assignments, strain histories and properties of pure cultures of cyanobacteria. J Gen Microbiol 111:1–61

Shao J, Wu Z, Yu G, Peng X, Li R (2009) Allelopathic mechanism of pyrogallol to *Microcystis aeruginosa* PCC7806 (Cyanobacteria): from views of gene expression and antioxidant system. Chemosphere 75:924–928

Shibata K (1969) Pigments and a UV-absorbing substance in corals and a blue-green alga living on the Great Barrier Reef. Plant Cell Physiol 10:325–335

Shick JM, Dunlap WC (2002) Mycosporine-like amino acids and related Gadusols: biosynthesis, accumulation, and UV-protective functions in aquatic organisms. Annu Rev Physiol 64:223–262

Singh SP, Kumari S, Rastogi RP, Singh KL (2008a) Mycosporine-like amino acids (MAAs): chemical structure, biosynthesis and significance as UV-absorbing/screening compounds. Indian J Exp Biol 46:7–17

Singh SP, Klisch M, Häder D-P, Sinha RP (2008b) Role of various growth media on shinorine (mycosporine-like amino acid) concentration and photosynthetic yield in *Anabaena variabilis* PCC 7937. World J Microbiol Biotechnol 24:3111–3115

Singh SP, Häder D-P, Sinha RP (2010) Cyanobacteria and ultraviolet radiation (UVR) stress: Mitigation strategies. Ageing Res Rev 9:79–290

Singh JS, Kumar A, Rai AN, Singh DP (2016) Cyanobacteria: a precious bio-resource in agriculture, ecosystem, and environmental sustainability. Front Microbiol 7:529

Singh A, Tyagi MB, Kumar A (2017a) Cyanobacteria growing on tree barks possess high amount of sunscreen compound mycosporine-like amino acids (MAAs). Plant Physiol Biochem 119:110–120

Singh DK, Richa, Kumar D, Chatterjee A, Rajneesh, Pathak J, Sinha RP (2017b) Response of the cyanobacterium *Fischerella* sp. strain HKAR-5 against combined stress of UV-B radiation, PAR and pyrogallic acid. JSM Environ Sci Ecol 5:1049

Singh DK, Pathak J, Pandey A, Singh V, Ahmed H, Kumar D, Sinha RP (2020a) Ultraviolet-screening compound mycosporine-like amino acids in cyanobacteria: biosynthesis, functions, and applications. In: Singh PK, Kumar A, Singh VK, Shrivastava AK (eds) Advances in cyanobacterial biology. Academic Press, New York, pp 219–233

Singh V, Pathak J, Pandey A, Kumar D, Ahmed H, Singh DK, Richa, Sinha RP (2020b) Mycosporine-like amino acids and antioxidative enzymes activity in *Scytonema* sp. under cumulative stress of UV radiation and salinity. J Sci Res 64:207–216

Singh DK, Pathak J, Pandey A, Singh V, Ahmed H, Kumar D, Rajneesh SRP (2021) Response of a rice-field cyanobacterium *Anabaena* sp. HKAR-7 upon exposure to ultraviolet-B radiation and ammonium chloride. Environ Sustain 4:95–105

Singh V, Pathak J, Pandey A, Ahmed H, Rajneesh KD, Sinha RP (2022) UV-induced physiological changes and biochemical characterization of mycosporine-like amino acid in a rice-field cyanobacterium *Fischerella* sp. strain HKAR-13. S Afr J Bot 147:81–97

Sinha RP, Häder D-P (2003) Biochemistry of mycosporine-like amino acids (MAAs) synthesis: role in photoprotection. Recent Res Dev Biochem 4:971–983

Sinha RP, Häder D-P (2008) UV protectants in cyanobacteria. Plant Sci 174:278–289

Sinha RP, Dautz M, Häder D-P (2001a) A simple and efficient method for the quantitative analysis of thymine dimers in cyanobacteria, phytoplankton and macroalgae. Acta Protozool 40:187–195

Sinha RP, Klisch M, Helbling EW, Häder D-P (2001b) Induction of mycosporine-like amino acids (MAAs) in cyanobacteria by solar ultraviolet-B radiation. J Photochem Photobiol B 60:129–135

Sinha RP, Singh SP, Häder D-P (2007) Database on mycosporines and mycosporine-like amino acids (MAAs) in fungi, cyanobacteria, macroalgae, phytoplankton and animals. J Photochem Photobiol B 89:29–35

Sonntag B, Summerer M, Sommaruga R (2007) Sources of mycosporine-like amino acids in planktonic *Chlorella*-bearing ciliates (Ciliophora). Freshw Biol 52:1476–1485

Stanier RY, Cohen-Bazire G (1977) Phototrophic prokaryotes: the cyanobacteria. Annu Rev Microbiol 31:225–274

Takano S, Uemura D, Hirata Y (1978) Isolation and structure of a new amino acid, palythine, from the zoanthid *Palythoa tuberculosa*. Tetrahedron Lett 26:2299–2300

Torres A, Enk CD, Hochberg M, Srebnik M (2006) Porphyra-334, a potential natural source for UVA protective sunscreens. Photochem Photobiol Sci 5:432–435

Upadhyay G, Gupta SP, Prakash O, Singh MP (2010) Pyrogallol-mediated toxicity and natural antioxidants: triumphs and pitfalls of preclinical findings and their translational limitations. Chem Biol Interact 183:333–340

Vanderstukken M, Mazzeo N, Van Colen W, Declerck SA, Muylaert K (2011) Biological control of phytoplankton by the subtropical submerged macrophytes *Egeria densa* and *Potamogeton illinoensis*: a mesocosm study. Freshw Biol 56:1837–1849

Waditee-Sirisattha R, Kageyama H, Sopun W, Tanaka Y, Takabe T (2014) Identification and upregulation of biosynthetic genes required for accumulation of mycosporine-2-glycine under salt stress conditions in the halotolerant cyanobacterium *Aphanothece halophytica*. Appl Environ Microbiol 80:1763–1769

Wang J, Zhu J, Liu S, Liu B, Gao Y, Wu Z (2011) Generation of reactive oxygen species in cyanobacteria and green algae induced by allelochemicals of submerged macrophytes. Chemosphere 85:977–982

Weatherhead EC, Andersen SB (2006) The search for signs of recovery of the ozone layer. Nature 441:39–45

Wu ZB, Deng P, Wu XH, Luo S, Gao YN (2007) Allelopathic effects of the submerged macrophyte *Potamogeton malaianus* on *Scenedesmus obliquus*. Hydrobiologia 592:465–474

Wu Z, Shi J, Yang S (2013) The effect of pyrogallic acid on growth, oxidative stress, and gene expression in *Cylindrospermopsis raciborskii* (Cyanobacteria). Ecotoxicology 22:271–278

Yoshiki M, Tsuge K, Tsuruta Y, Yoshimura T, Koganemaru K, Sumi T, Matsui T, Matsumoto K (2009) Production of new antioxidant compound from mycosporine-like amino acid, porphyra-334 by heat treatment. Food Chem 113:1127–1132

Zhu J, Liu B, Wang J, Gao Y, Wu Z (2010) Study on the mechanism of allelopathic influence on cyanobacteria and chlorophytes by submerged macrophyte (*Myriophyllum spicatum*) and its secretion. Aquat Toxicol 98:196–203